Yamagata K, Zhao Y, Kouzmenko A, et al. (2004) A novel genetic system for analysis of co-activators for the N-terminal transactivation function domain of the human androgen receptor. *Biosci Biotechnol Biochem* **68:**1209–1215.

Takeyama K, Ito S, Yamamoto A, Tanimoto H, Furutani T, Kanuka H, Miura M, Tabata T, and Kato S (2002) Androgen-dependent neurodegeneration by polyglutamine-expanded human androgen receptor in Drosophila. *Neuron* **35:**855–864.

Takeyama K, Masuhiro Y, Fuse H, Endoh H, Murayama A, Kitanaka S, Suzawa M, Yanagisawa J, and Kato S (1999) Selective interaction of vitamin D receptor with transcriptional coactivators by a vitamin D analog. *Mol Cell Biol* **19:**1049–1055.

Tanimoto H, Itoh S, ten Dijke P, and Tabata T (2000) Hedgehog creates a gradient of DPP activity in Drosophila wing imaginal discs. *Mol Cell* **5:**59–71.

Tsuneizumi K, Nakayama T, Kamoshida Y, Kornberg TB, Christian JL, and Tabata T (1997) Daughters against dpp modulates dpp organizing activity in Drosophila wing development. *Nature (Lond)* **389:**627–631.

Watanabe M, Yanagisawa J, Kitagawa H, Takeyama K, Ogawa S, Arao Y, Suzawa M, Kobayashi Y, Yano T, Yoshikawa H, et al. (2001) A subfamily of RNA-binding DEAD-box proteins acts as an estrogen receptor alpha coactivator through the N-terminal activation domain (AF-1) with an RNA coactivator, SRA. *EMBO (Eur Mol Biol Organ) J* **20:**1341–1352.

Wilson JD (1999) The role of androgens in male gender role behavior. *Endocr Rev* **20:**726–737.

Yanagisawa J, Kitagawa H, Yanagida M, Wada O, Ogawa S, Nakagomi M, Oishi H, Yamamoto Y, Nagasawa H, McMahon SB, et al. (2002) Nuclear receptor function requires a TFTC-type histone acetyl transferase complex. *Mol Cell* **9:**553–562.

Yeh S and Chang C (1996) Cloning and characterization of a specific coactivator, ARA70, for the androgen receptor in human prostate cells. *Proc Natl Acad Sci USA* **93:**5517–5521.

Address correspondence to: Shigeaki Kato, Institute of Molecular and Cellular Biosciences, The University of Tokyo, Yayoi 1-1-1, Bunkyo-ku, Tokyo 113-0032, Japan. E-mail: uskato@mail.ecc.u-tokyo.ac.jp

Repressive domain of unliganded human estrogen receptor α associates with Hsc70

Satoko Ogawa[1], Hajime Oishi[1], Yoshihiro Mezaki[1], Madoka Kouzu-Fujita[1], Reiko Matsuyama[1], Madoka Nakagomi[1], Eri Mori[1], Emi Murayama[2], Hiromichi Nagasawa[2], Hirochika Kitagawa[1], Junn Yanagisawa[1], Tetsu Yano[3] and Shigeaki Kato[1,4,*]

[1]*The Institute of Molecular and Cellular Biosciences, University of Tokyo, 1-1-1 Yayoi, Bunkyo-ku, Tokyo, 113-0032, Japan*
[2]*Department of Applied Biological Chemistry, Graduate School of Agricultural and Life Sciences, University of Tokyo, 1-1-1 Yayoi, Bunkyo-ku, Tokyo, 113-0032, Japan*
[3]*Department of Obstetrics and Gynecology, University of Tokyo, Hongo 7-3-1, Bunkyo-ku, Tokyo 113-8655, Japan*
[4]*ERATO, Japan Science and Technology Agency, 4-1-8 Honcho, Kawaguchi, Saitama, 332-0012, Japan*

Estrogen receptor (ER) is a hormone-inducible transcription factor as a member of the nuclear receptor gene superfamily. Unliganded ER is transcriptionally silent and capable of DNA binding; however, it is unable to suppress the basal activity of the target gene promoters, unlike non-steroid hormone receptors that associate with corepressors in the absence of their cognate ligands. To study the molecular basis of how unliganded human ERα is maintained silent in gene regulation upon the target gene promoters, we biochemically searched interactants for hERα, and identified heat shock protein 70 (Hsc70). Hsc70 appeared to associate with the N-terminal hormone binding E domain, that also turned out a transcriptionally repressive domain. Competitive association of Hsc70 with a best known coactivator p300 was observed. Thus, these findings suggest that Hsc70 associates with unliganded hERα, and thereby deters hERα from recruiting transcriptional coregulators, presumably as a component of chaperone complexes.

Introduction

A wide variety of estrogen action is mediated through the transcriptional control of target genes by nuclear estrogen receptor (ER) (Couse & Korach 1999; Ciana *et al.* 2003). Two known subtypes of ER, α and β, belong to the nuclear receptor superfamily and act as ligand-induced transcription factors. Like in other nuclear receptor superfamily members, structure of the ER proteins is divided into five or six functional domains (designated as A to E/F domains) (Mangelsdorf *et al.* 1995). The highly conserved DNA binding domain is located in the C domain, while the ligand-binding domain (LBD) is mapped to the E/F domain. Ligand binding causes a conformational change with dramatic shifting of the helix 12. In the ER, transactivation function is present in the N-terminal A/B domain (AF-1) and in the C-terminal LBD (AF-2) (Kumar *et al.* 1987; Tora *et al.* 1989). Although both AF-1 and AF-2 are involved in the ligand-dependent transactivation function of the ER, AF-1 is constitutively active, while AF-2 activity is dependent on the ligand binding (Endoh *et al.* 1999; Kobayashi *et al.* 2000; Watanabe *et al.* 2001).

ER target gene promoters contain estrogen response elements (EREs) that are recognized and directly bound by ER homo- or hetero-dimers followed by chromatin remodeling, presumably by recruited ATP-dependent chromatin remodeling complexes (Belandia & Parker 2003; Kitagawa *et al.* 2003). ERE bound liganded ERs also recruit a number of histone acetyltransferases (HATs) and non-HAT cofactors that further enhance transcription (McKenna & O'Malley 2002). HAT coactivator complexes, CBP/p160 (Onate *et al.* 1995; Kamei *et al.* 1996; Chen *et al.* 1997; Spencer *et al.* 1997) and TRRAP/GCN5 (Yanagisawa *et al.* 2002), and non-HAT DRIP/TRAP complexes (Fondell *et al.* 1996; Yuan *et al.* 1998; Naar *et al.* 1999; Rachez *et al.* 1999) are thought to act as common coactivator complexes for ERs as well as for other DNA-binding transcription factors. Thus, ligand-induced conformational alteration switches ER from transcriptionally suppressed into

Communicated by: Kohei Miyazono
**Correspondence*: E-mail: uskato@mail.ecc.u-tokyo.ac.jp

DOI: 10.1111/j.1365-2443.2005.00904.x

transcriptionally active state via the recruitment of coactivators (Freedman 1999; Glass & Rosenfeld 2000; Metivier *et al.* 2003). Despite identification of a large number of factors/complexes that coactivate the ER function, a factor/complex that associates with unliganded ERs and suppresses their transactivation function remains to be identified. Although several HDAC complexes containing NCoR/SMART or sin3A (Kurokawa *et al.* 1995; Nagy *et al.* 1997) have been reported to be recruited by synthetic estrogen antagonist-bound ERs (Jepsen *et al.* 2000; Yamamoto *et al.* 2001), HDAC complexes are unlikely to render unliganded ERs suppressive in gene regulations even though unliganded ERs are bound to EREs, since unliganded ERs are unable to suppress the basal activity of the target gene promoters. Considering recent findings that eight classes of nuclear complexes are differentially and temporally recruited to ERE bound ERs (Metivier *et al.* 2003), it is feasible that unliganded ERs also associate with some cytosolic and/or nuclear factors/complexes.

To address this issue, this study has been undertaken to identify an ERα interactant that renders ERα inactive in transactivation. As unliganded ERα is transcriptionally inactive, first we have mapped a molecular region in its structure that is involved in suppression of the basal transcriptional activity of the wild-type ERα. A segment in the ERα LBD N-terminal region has been identified as repression domain (ERα RD). To search for proteins interacting with unliganded ERα, we used HeLa cell nuclear extract that is known to contain major, if not all, coactivator complexes to support the transactivation function of the liganded ERα. Using some of the modern biochemical techniques, we have identified heat shock protein 70 (Hsc70) as a factor that physically associates with the ERα RD *in vivo* and *in vitro*. Thus, the present study indicates that a chaperone complex containing Hsc70 associates with the unliganded ERα, thereby prevents ERα from recruitment of coactivators and renders the receptor transcriptionally silent.

Results

Mapping of a repression domain of human estrogen receptor α

Human estrogen receptors (hERs) are well known to be transcriptionally silent when ligand is unbound irrespective of DNA binding. Although other members of nuclear receptor superfamily, like retinoid receptors (RAR/RXR) and thyroid hormone receptor (TR), are potent repressors of basal transcriptional activity of the target promoters in the absence of cognate ligands (Kurokawa *et al.* 1995; Nagy *et al.* 1997), unliganded ERs are shown not to exhibit such suppressive function. It is, therefore, most likely that unliganded ERs associate with transcriptionally neutral factors, that attenuate the transactivation function of the N- and C-terminal domains (AF-1 and AF-2) of ERs.

To test this hypothesis, we first mapped a transrepressive region in the human ERα using a series of hERα deletion mutants (Fig. 1A) in a transient expression assay in HeLa cells with a luciferase reporter gene harboring consensus ERE in the promoter. As expected from the previous findings that the N-terminal AF-1 domain is ligand-independent in transactivation, the mutants lacking the LBD [ERα(1-288)] were active in transcription (Fig. 1B). The AF-2 function in the LBD appeared intact to confer estrogen responsiveness in the mutants retaining the LBD (Fig. 1B). The D domain itself appeared to have no transactivation function; however, the vicinal LBD region (340-396 amino acids) was rather suppressive for the AF-1 function (Fig. 1B). Together with a further C-terminal extention (396-461 a.a.), these two regions together (340-461 a.a.) appeared to act as a repression domain for the AF-1 domain. We therefore addressed this possibility by deleting only these regions (see ERα(Δ341-396) and ERα(Δ341-461)) and indeed, found that only the mutant lacking of both regions acquired ligand-independent transactivation function, clearly confirming that the region between 341 and 461 a.a. (designated as hERα Repression Domain) is capable of inhibiting the hERα AF-1 function in the A/B domain. To verify the AF-1 function in the hERα (Δ341-461) mutant, transcriptional effect of the p300 HAT coactivator on this mutant was examined (Fig. 1C). p300 has been already reported to coactivate both AF-1 and AF-2 functions (Kobayashi *et al.* 2000; Watanabe *et al.* 2001), and consistently it potentiated the transactivation function of the tested hERα mutants. Thus, even though the ligand is unbound, the AF-1 A/B domain is apparently exposed for recruitment of coactivators like p300 when the RD domain is deleted from the hERα.

The RD domain associates with a protein factor

To address the question of whether the RD domain harbors a transrepressive function or alters hERα secondary structure to render the receptor inactive in transactivation, the function of the RD was examined in the mammalian two-hybrid system assay using GAL4 DNA binding domain-fused chimeric hERα mutants and transcriptional activator VP16 fusion constructs (Fig. 2). The AF-1 function of the hERα deletion mutant [ERα(1-461)] is inactive due to the presence of RD domain, and

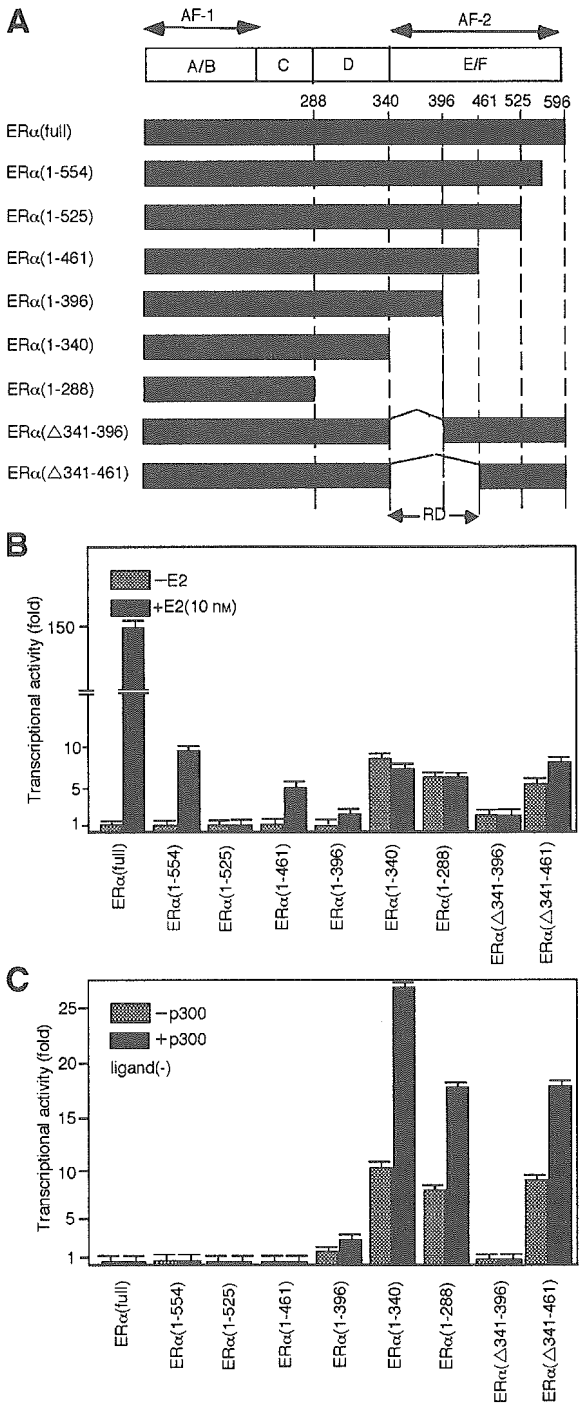

Figure 1 Mapping of a repression domain (RD) of human estrogen receptor α (hERα). (A) Schematic representation of hERα deletion mutants. The DNA binding domain (DBD) is located in the C domain. The transactivation function-1 (AF-1) region is located in the N-terminal A/B domain, while the transactivation function-2 (AF-2) region is located in the C-terminal E/F domain that also contains the ligand binding domain (LBD). All deletion constructs are inserted in pcDNA3 plasmid. (B, C) Measurement of hERα mutant constructs transactivation in HeLa cells. (B) HeLa cells were transfected with hERα mutant expression plasmids, ERE-tk-luc reporter plasmids and pRL-CMV internal control plasmids in the presence or absence of 10^{-8} M E2. Firefly luciferase activity (pRL-ERE-tk-luc) was measured and normalized against Renilla activity (pRL-CMV-luc) as an internal control. (C) HeLa cells were transfected with hERα mutant expression plasmids, ERE-tk-luc reporter plasmids and pRL-CMV internal control plasmids in the presence or absence of p300 expression plasmids (pcDNA3-p300). All values are means ± SEM.

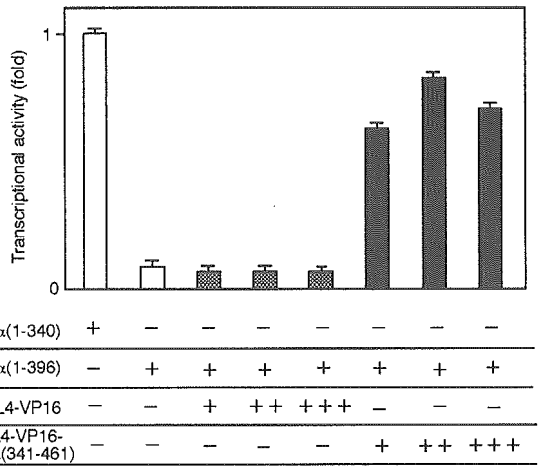

Figure 2 Transcriptional squelching in the RD domain of hERα. RD domain fused to GAL4-VP16 chimeric protein squelches the RD function of hERα and stimulates transcription. HeLa cells were transfected with hERα(1-340) or hERα(1-396) and GAL4-VP16 or GAL4-VP16-hERα(341-461) expression plasmids. ERE-tk-luc reporter plasmids and pRL-CMV internal control plasmids were used and luciferase activity was measured as described in Fig. 1 (B, C). (+: 10 ng, ++: 50 ng, +++: 250 ng.)

GAL4-VP16 expectedly had no effect on the transactivation of this hERα mutant. However, when GAL4-VP16 was fused with the RD domain [GAL4-VP16-ER(341-461)], this fusion protein was capable of stimulating transcriptional activity of hERα(1-461), suggesting that the RD domain fused to GAL4-VP16 fusion protein quashes the RD function (Fig. 2). Considering that even a most potent activator, VP16, by itself did not interfere with the transactivation function of hERα(1-340) by competing with the recruitment of coactivators, it is most likely that the RD domain associates with a transcriptionally neutral protein factor.

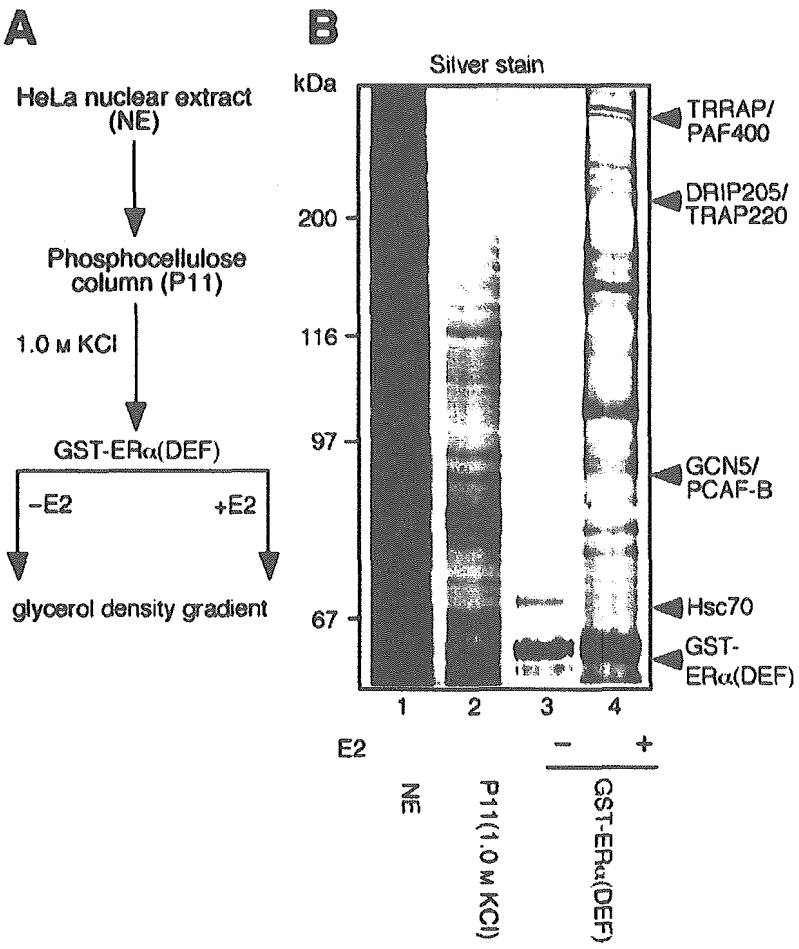

Figure 3 Identification of Hsc70 as an interactant for unliganded hERα. (A) Biochemical purification strategy. HeLa nuclear extracts were loaded onto a P11 phosphocellulose column. Bound proteins were eluted by 1.0 M KCl elution buffer. Bead-immobilized GST-hERα(LBD) proteins were then incubated with P11 column-eluted fractions in the absence or presence of 10^{-6} M E2. Complexes bound to the unliganded or liganded hERα were eluted with reduced glutathione. (B) SDS-PAGE followed by silver staining of the nuclear extract (lane 1), eluate from P11 column (lane 2), purified proteins from glycerol density gradient in the absence or presence of E2 (lanes 3, 4). Hsc70 was identified as an unliganded hERα by TOF-MS.

Identification of heat shock protein p70 as an interactant for the unliganded hERα

To identify an unliganded ERα RD-interacting protein(s), we have undertaken a biochemical approach to purify from HeLa nuclear extract factors and complexes associating with the hERα (Fig. 3A). As we have previously reported, a number of factors like TFTC-type HAT complex components were trapped by the hERα only in the presence of E2 (Yanagisawa *et al.* 2002), confirming our purification of ligand-dependent interactants (Fig. 3A). Only a few proteins bound to unliganded hERα were detected, and one of them was identified by TOF-MS as heat shock protein p70 (Hsc70) (Ballinger *et al.* 1999; Alberti *et al.* 2002) that was undetectable in fractions purified with liganded hERα (Fig. 3B). To verify the Hsc70 association with unliganded hERα, co-immunoprecipitation was performed from HeLa cells (Fig. 4). Endogenous Hsc70 was co-immunoprecipitated with hERα only when the cells were untreated with E2 (Fig. 4A). Furthermore, Hsc70 association with hERα required RD domain (Fig. 4B). Thus, these findings suggest that Hsc70 dissociates from hERα upon estrogen binding, releasing hERα from its suppressive action.

Repression of the unliganded ERα transactivation function through the RD domain is a nuclear event

To exclude the possibility that the transrepressive function of the RD domain towards the AF-1 and AF-2 is coupled with simply an extranuclear event, cellular localization of the hERα mutants was examined (Fig. 5). As expected from the previous reports, wild-type hERα mainly localized in the nuclei irrespective of E2 binding, and partial cytoplasmic localization of hERα indicated the intracellular shuffling (Watanabe *et al.* 2001). In accordance with the previous findings that, similar to other nuclear receptors, major nuclear localization signal (NLS) is present in the hERα hinge D domain (256-303 a.a.) (Ylikomi *et al.* 1992), all of the tested mutants retaining

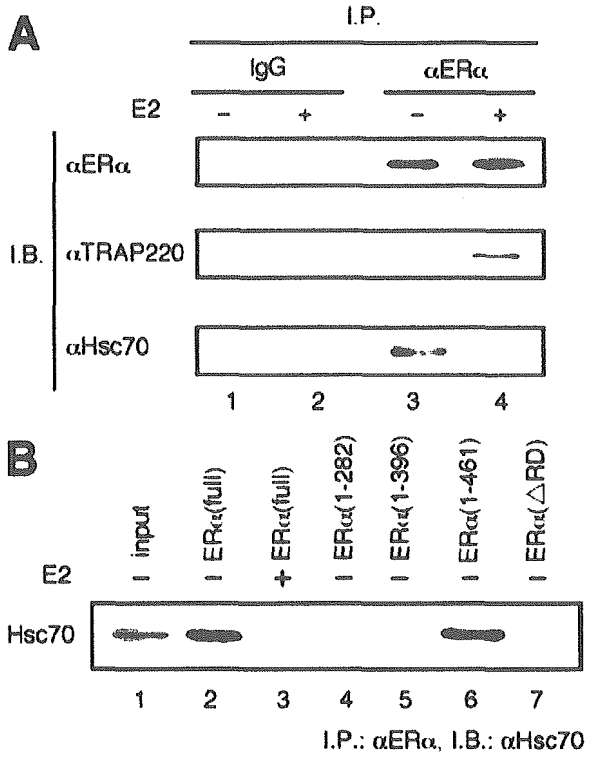

Figure 4 Hsc70 associates with unliganded hERα. (A) MCF7 cells were treated with or without E2 and whole-cell extracts were immunoprecipitated with anti-hERα antibody or irrelevant (nonspecific control) antibodies, followed by Western blotting with anti-hERα antibody, anti-TRAP220 antibody or anti-Hsc70 antibody. (B) HeLa cells were transfected with hERα deletion constructs. Whole-cell extracts were immunoprecipitated with anti-hERα antibody and detected by Western blotting with anti-Hsc70 antibody.

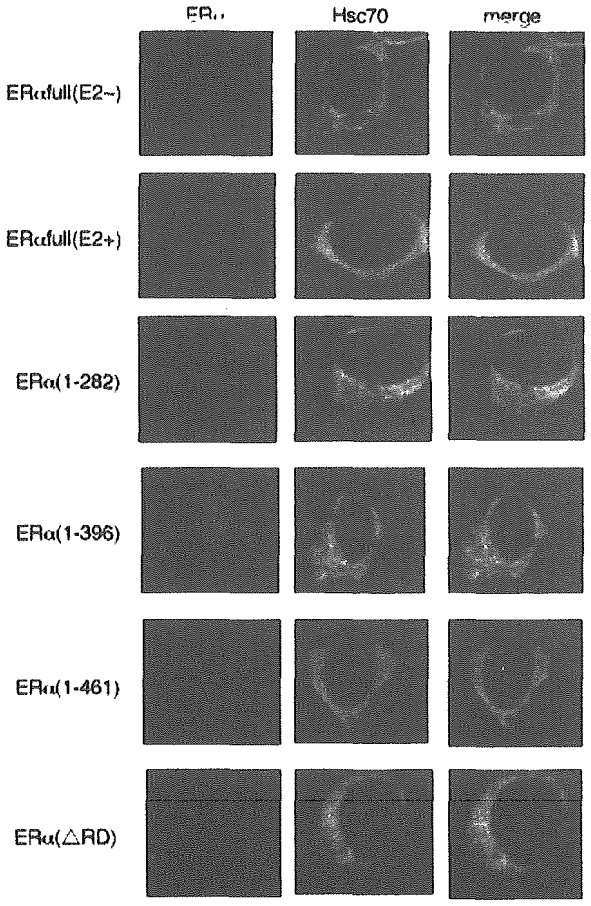

Figure 5 Cellular localization of the hERα mutants (red) and Hsc70 (green). HeLa cells were transfected with hERα deletion constructs and GFP-Hsc70 fusion constructs. hERα mutant localization was observed with anti-hERα antibody (red) and Hsc70 localization was monitored as GFP fusion protein (green). Hsc70 localization was mainly in the cytoplasm, but in the presence of unliganded hERα and hERα mutants retaining the RD, nuclear localization of Hsc70 can be observed.

the D domain were predominantly localized in the nucleus, and the hERα(Δ341-461) mutant was indistinguishable from the wild-type hERα in intracellular localization. Hsc70 localization was monitored as a GFP fusion protein, and was located mainly in the cytoplasm. However, in the presence of unliganded hERα and hERα mutants retaining the RD, albeit as a weak signal, nuclear localization of Hsc70 has also been detected (Fig. 5). Thus, from these findings it is apparent that the function of the hERα RD is coupled with neither extranuclear localization nor intracellular shuffling.

Hsc70 competes with HAT co-activator p300 for association with ER

Finally, to explore the possible mechanism of how Hsc70 renders unliganded hERα inactive in transactivation, associations of the Hsc70 and best characterized HAT coactivator p300 with hERα were examined by co-immunoprecipitation (Fig. 6). Reflecting coactivation of the hERα mutants by p300, association of p300 with the mutants was detected without Hsc70 interaction. Reversely, Hsc70 was co-immunopreceipitated by the hERα mutants harboring the RD, without p300 association. Thus, although Hsc70 itself seems to have no modulatory activity in transcriptional regulation, the association of Hsc70 with hERα appears to prevent hERα from coactivator recruitment, and Hsc70 is presumed to be dissociated from hERα upon liganded binding.

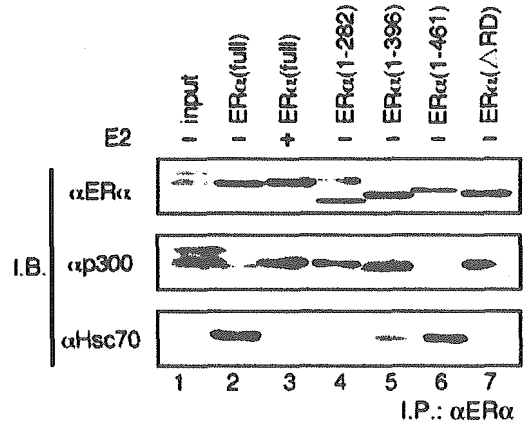

Figure 6 Hsc70 and p300 compete for binding to hERα. HeLa cells were transfected with hERα deletion mutants and whole-cell extracts were immunoprecipitated with anti-hERα antibody followed by Western blotting using anti-hERα antibody, anti-p300 antibody or anti-Hsc70 antibody.

Discussion

Identification of repression domain (RD) in human ERα

Like some other members of the nuclear receptor superfamily, unliganded hERα is transcriptionally inactive *in vivo* and *in vitro* even when hERα is stably bound to its target DNA elements refereed as estrogen response elements (EREs). Steroid hormone receptors, including hERα, are distinct from the RXR-heterodimerized non-steroid hormone receptors, like thyroid hormone receptors (TRs), all-trans retinoic acid receptors (RARs) and vitamin D receptor (VDR), in terms of the transcriptional function of unliganded receptors bound to their cognate target gene promoters. These non-steroid hormone receptors are known to suppress the basal transcriptional activity of their target gene promoters in the absence of cognate ligands, and this led to the identification of a number of corepressors and corepressor complexes that often comprise histone deacetylases (HDAC) to convert transcriptionally active chromatin into inactive by histone deacetylation (Kurokawa *et al.* 1995; Nagy *et al.* 1997). However, these HDAC-containing complexes have been reported not to associate with unliganded steroid receptors (Kurokawa *et al.* 1995; Nagy *et al.* 1997; Yamamoto *et al.* 2001), reflecting the facts that unliganded steroid receptors are unable to suppress the basal transcriptional activity of target gene promoters. Thus, it is likely that a transcriptionally neutral factor may associate with unliganded steroid receptors through the repression domains to maintain receptors inactive in gene regulations. To address this possibility, we have identified a domain responsible for such inactivation of the receptor function. In hERα, a repression domain (RD) was localized in the N-terminal region of the LBD. This repression domain is located close to the helix12 that shifts upon ligand binding to the receptor (Shiau *et al.* 2002; Wu *et al.* 2005), and it is therefore possible to suggest that this conformational change or subsequent recruitment of coactivator complexes may induce dissociation of a factor associated with the RD.

Hsc70 as an interactant for the hERα RD

Following this hypothesis, we biochemically purified interactants for unliganded hERα and found that in comparison with the ligand-bound hERα, substantially fewer factors were associated with the unliganded receptor. Using a number of independent methods, we identified Hsc70 as an interactant for the hERα RD. Since Hsc70 is a component of a chaperone complex (Ballinger *et al.* 1999; Alberti *et al.* 2002), an Hsc70-containing chaperone complex appears to associate with the hERα. In Fig. 6, we demonstrated that p300 association with hERα is switched with Hsc70 by estrogen binding, and similarly we observed such hormone-induced switching with the p160 member coactivators (data not shown). Thus, this association may reflect an 'inactive form' of hERα, presumably preventing physical interactions of a number of coactivators/complexes to hERα AF-1 and AF-2. Another chaperone complex containing Hsc90 has been known to associate with steroid receptors in cytoplasm (Picard *et al.* 1990). Similar to Hsc90, Hsc70 also has a predominant cytoplasmic localization, whereas the hERα appears to predominantly localize in the nucleus irrespective of presence of ligand. In this study we have provided evidence that Hsc70 associates with unliganded hERα in the nucleus.

Recently, CHIP has been identified as a component of a ubiquitin ligase complex that ubiquitinates and thereby promotes degradation of unliganded hERα (Tateishi *et al.* 2004). Interestingly, this CHIP complex is presumed to selectively degrade misfolded hERα molecules in the cytoplasm and contains Hsc70 and other Hsc proteins. CHIP is thus likely to control the quality of hERα protein, and may associate with the Hsc70 containing chaperone complex together with BAG-1 when required (Alberti *et al.* 2002). Thus, Hsc70 appears to physically interact with unliganded hERα as a unit of the chaperone complex and act as a modulator in regulation of the transactivation function and quality control of hERα as well as other not yet identified receptor functions.

Experimental procedures

Purification and separation of ERα-associated complexes

HeLa nuclear extracts were loaded onto a P11 phosphocellulose column (Yanagisawa *et al.* 2002; Kitagawa *et al.* 2003). After extensive washing with washing buffer (20 mM Tris-HCl pH 7.9, 150 mM KCl, 0.2 mM EDTA, 0.05% NP40, 10% glycerol, 0.5 mM PMSF, 1 mM DTT), bound proteins were eluted by elution buffer (20 mM Tris-HCl pH 7.9, 1 M KCl, 0.2 mM EDTA, 0.05% NP40, 10% glycerol, 0.5 mM PMSF, 1 mM DTT). Immobilized GST-ERα LBD fusion proteins were preincubated for 1 h at 4 °C in GST-binding buffer (20 mM Tris-HCl pH 7.9, 180 mM KCl, 0.2 mM EDTA, 0.05% NP40, 0.5 mM PMSF, 1 mM DTT) containing BSA (1 mg/mL) and E_2 (10^{-6} M). Bead-immobilized proteins were then incubated at 4 °C for 6–10 h with P11 column-eluted fractions in the presence of 10^{-6} M E_2. After washing with GST wash buffer (GST-binding buffer with 0.1% NP-40) three times, the beads were further washed with a GST wash buffer containing 0.2% *N*-lauroyl sarkosine (Sarkosyl, Sigma). Complexes associated with E_2-bound or unliganded ERα were eluted with 15 mM reduced glutathione in elution buffer (50 mM Tris-HCl pH 8.3, 150 mM KCl, 0.5 mM EDTA, 0.5 mM PMSF, 5 mM NaF, 0.08% NP-40, 0.5 mg/mL BSA, and 10% glycerol). For fractionation on glycerol gradient, elutants were layered onto the top of a 4.5 mL linear 100–40% glycerol gradient in GST-binding buffer and centrifuged for 16 h at 4 °C at 40 000 r.p.m. in a SW40 rotor (Beckman). Protein standards used were ovalbumin (44 kDa); β-globulin (158 kDa); and thyroglobulin (667 kDa) (Watanabe *et al.* 2001).

GST pull-down assay

GST-fusion proteins were expressed in *Escherichia coli*, and bound to glutathione-sepharose 4B beads (Pharmacia Biotech) (Yanagisawa *et al.* 2002). The *in vitro* translated proteins were then incubated with beads in NET-N buffer (20 mM Tris-HCl pH 7.5, 200 mM NaCl, 1 mM EDTA, 0.5% NP40) with 1 mM PMSF. Bound proteins were separated by 7.5% SDS-PAGE, lightly stained with Coomasie Brilliant Blue to verify equal amounts of fusion protein, and then visualized by autoradiography (Endoh *et al.* 1999).

Immunoprecipitation

After washing MCF7 cells twice with ice-cold phosphate-buffered saline, the collected cells were resuspended in 1 mL ice-cold lysis buffer (10 mM Tris-HCl pH 7.5, 10 mM NaCl, 3 mM $MgCl_2$, 0.5% NP40), incubated on ice for 30 min, then centrifuged again for 5 min at 500 ***g***. Sedimented nuclear fractions were resuspended in TNE buffer (10 mM Tris-HCl pH 7.5, 0.15 M NaCl, 1 mM EDTA, 1% NP40) and incubated for 30 min on ice. After centrifugation, the supernatants were used as MCF7 whole-cell extracts for immunoprecipitation using anti-hERα antibody (anti-ERα Ab-1; NEO MARKERS) followed by Western blotting using anti-ERα antibody, anti-TRAP220 antibody (Santa Cruz Biotechnology), or anti-Hsc70 antibody raised against the N-terminal region (Santa Cruz Biotechnology) (Yanagisawa *et al.* 1999).

Transfection and luciferase assay

Cells at 40–50% confluence were transfected with the indicated plasmids using Lipofectamine regent (Gibco BRL) in 12-well Petri dishes (Ito *et al.* 2004). Total amounts of DNA were adjusted by supplementing with empty vector up to 1.0 μg. Luciferase activity was determined using the Luciferase Assay System (Promega). As a reference plasmid to normalize transfection efficiency, 25 ng of pRL-CMV plasmid (Promega) was co-transfected in all experiments (Takeyama *et al.* 1999).

Histology

HeLa cells were transfected with hERα constructs and GFP-Hsc70 plasmids. The cells were fixed for 20 min in 4% formaldehyde at 25 °C and were incubated with primary antibody B10 that recognize the N-terminal regions of hERα. Cy3-conjugated anti-mouse IgG was used as a secondary antibody for immunofluorescence staining. hERα and GFP expression were detected using a Zeiss Confocal Laser Scanning System 510.

Acknowledgements

We thank Prof P. Chambon for hERα expression vectors and anti-hERα antibody (B10) and H. Higuchi for manuscript preparation. This work was supported by a grant-in-aid for priority areas from the Ministry of Education, Science, Sports and Culture of Japan (K.T. and S.K.) and Basic Research Activities for Innovative Biosciences (BRAIN) (S.K.).

References

Alberti, S., Demand, J., Esser, C., Emmerich, N., Schild, H. & Hohfeld, J. (2002) Ubiquitylation of BAG-1 suggests a novel regulatory mechanism during the sorting of chaperone substrates to the proteasome. *J. Biol. Chem.* **277**, 45920–45927.

Ballinger, C.A., Connell, P., Wu, Y., *et al.* (1999) Identification of CHIP, a novel tetratricopeptide repeat-containing protein that interacts with heat shock proteins and negatively regulates chaperone functions. *Mol. Cell. Biol.* **19**, 4535–4545.

Belandia, B. & Parker, M.G. (2003) Nuclear receptors: a rendezvous for chromatin remodeling factors. *Cell* **114**, 277–280.

Chen, H., Lin, R.J., Schiltz, R.L., *et al.* (1997) Nuclear receptor coactivator ACTR is a novel histone acetyltransferase and forms a multimeric activation complex with P/CAF and CBP/p300. *Cell* **90**, 569–580.

Ciana, P., Raviscioni, M., Mussi, P., *et al.* (2003) In vivo imaging of transcriptionally active estrogen receptors. *Nature Med.* **9**, 82–86.

Couse, J.F. & Korach, K.S. (1999) Estrogen receptor null mice: what have we learned and where will they lead us? *Endocr. Rev.* **20**, 358–417.

Endoh, H., Maruyama, K., Masuhiro, Y., *et al.* (1999) Purification and identification of p68 RNA helicase acting as a transcriptional coactivator specific for the activation function 1 of human estrogen receptor alpha. *Mol. Cell. Biol.* **19**, 5363–5372.

Fondell, J.D., Ge, H. & Roeder, R.G. (1996) Ligand induction of a transcriptionally active thyroid hormone receptor coactivator complex. *Proc. Natl. Acad. Sci. USA* **93**, 8329–8333.

Freedman, L.P. (1999) Increasing the complexity of coactivation in nuclear receptor signaling. *Cell* **97**, 5–8.

Glass, C.K. & Rosenfeld, M.G. (2000) The coregulator exchange in transcriptional functions of nuclear receptors. *Genes Dev.* **14**, 121–141.

Ito, S., Takeyama, K., Yamamoto, A., *et al.* (2004) In vivo potentiation of human oestrogen receptor alpha by Cdk7-mediated phosphorylation. *Genes Cells* **9**, 983–992.

Jepsen, K., Hermanson, O., Onami, T.M., *et al.* (2000) Combinatorial roles of the nuclear receptor corepressor in transcription and development. *Cell* **102**, 753–763.

Kamei, Y., Xu, L., Heinzel, T., *et al.* (1996) A CBP integrator complex mediates transcriptional activation and AP-1 inhibition by nuclear receptors. *Cell* **85**, 403–414.

Kitagawa, H., Fujiki, R., Yoshimura, K., *et al.* (2003) The chromatin-remodeling complex WINAC targets a nuclear receptor to promoters and is impaired in Williams syndrome. *Cell* **113**, 905–917.

Kobayashi, Y., Kitamoto, T., Masuhiro, Y., *et al.* (2000) p300 mediates functional synergism between AF-1 and AF-2 of estrogen receptor alpha and beta by interacting directly with the N-terminal A/B domains. *J. Biol. Chem.* **275**, 15645–15651.

Kumar, V., Green, S., Stack, G., Berry, M., Jin, J.R. & Chambon, P. (1987) Functional domains of the human estrogen receptor. *Cell* **51**, 941–951.

Kurokawa, R., Soderstrom, M., Horlein, A., *et al.* (1995) Polarity-specific activities of retinoic acid receptors determined by a co-repressor. *Nature* **377**, 451–454.

Mangelsdorf, D.J., Thummel, C., Beato, M., *et al.* (1995) The nuclear receptor superfamily: the second decade. *Cell* **83**, 835–839.

McKenna, N.J. & O'Malley, B.W. (2002) Combinatorial control of gene expression by nuclear receptors and coregulators. *Cell* **108**, 465–474.

Metivier, R., Penot, G., Hubner, M.R., *et al.* (2003) Estrogen receptor-alpha directs ordered, cyclical, and combinatorial recruitment of cofactors on a natural target promoter. *Cell* **115**, 751–763.

Naar, A.M., Beaurang, P.A., Zhou, S., Abraham, S., Solomon, W. & Tjian, R. (1999) Composite co-activator ARC mediates chromatin-directed transcriptional activation. *Nature* **398**, 828–832.

Nagy, L., Kao, H.Y., Chakravarti, D., *et al.* (1997) Nuclear receptor repression mediated by a complex containing SMRT, mSin3A, and histone deacetylase. *Cell* **89**, 373–380.

Onate, S.A., Tsai, S.Y., Tsai, M.J. & O'Malley, B.W. (1995) Sequence and characterization of a coactivator for the steroid hormone receptor superfamily. *Science* **270**, 1354–1357.

Picard, D., Khursheed, B., Garabedian, M.J., Fortin, M.G., Lindquist, S. & Yamamoto, K.R. (1990) Reduced levels of hsp90 compromise steroid receptor action in vivo. *Nature* **348**, 166–168.

Rachez, C., Lemon, B.D., Suldan, Z., *et al.* (1999) Ligand-dependent transcription activation by nuclear receptors requires the DRIP complex. *Nature* **398**, 824–828.

Shiau, A.K., Barstad, D., Radek, J.T., *et al.* (2002) Structural characterization of a subtype-selective ligand reveals a novel mode of estrogen receptor antagonism. *Nature Struct. Biol.* **9**, 359–364.

Spencer, T.E., Jenster, G., Burcin, M.M., *et al.* (1997) Steroid receptor coactivator-1 is a histone acetyltransferase. *Nature* **389**, 194–198.

Takeyama, K., Masuhiro, Y., Fuse, H., *et al.* (1999) Selective interaction of vitamin D receptor with transcriptional coactivators by a vitamin D analog. *Mol. Cell. Biol.* **19**, 1049–1055.

Tateishi, Y., Kawabe, Y., Chiba, T., *et al.* (2004) Ligand-dependent switching of ubiquitin-proteasome pathways for estrogen receptor. *EMBO J.* **23**, 4813–4823.

Tora, L., White, J., Brou, C., *et al.* (1989) The human estrogen receptor has two independent nonacidic transcriptional activation functions. *Cell* **59**, 477–487.

Watanabe, M., Yanagisawa, J., Kitagawa, H., *et al.* (2001) A subfamily of RNA-binding DEAD-box proteins acts as an estrogen receptor alpha coactivator through the N-terminal activation domain (AF-1) with an RNA coactivator, SRA. *EMBO J.* **20**, 1341–1352.

Wu, Y.L., Yang, X., Ren, Z., *et al.* (2005) Structural basis for an unexpected mode of SERM-mediated ER antagonism. *Mol. Cell* **18**, 413–424.

Yamamoto, Y., Wada, O., Suzawa, M., *et al.* (2001) The tamoxifen-responsive estrogen receptor alpha mutant D351Y shows reduced tamoxifen-dependent interaction with corepressor complexes. *J. Biol. Chem.* **276**, 42684–42691.

Yanagisawa, J., Kitagawa, H., Yanagida, M., *et al.* (2002) Nuclear receptor function requires a TFTC-type histone acetyl transferase complex. *Mol. Cell* **9**, 553–562.

Yanagisawa, J., Yanagi, Y., Masuhiro, Y., *et al.* (1999) Convergence of transforming growth factor-beta and vitamin D signaling pathways on SMAD transcriptional coactivators. *Science* **283**, 1317–1321.

Ylikomi, T., Bocquel, M.T., Berry, M., Gronemeyer, H. & Chambon, P. (1992) Cooperation of proto-signals for nuclear accumulation of estrogen and progesterone receptors. *EMBO J.* **11**, 3681–3694.

Yuan, C.X., Ito, M., Fondell, J.D., Fu, Z.Y. & Roeder, R.G. (1998) The TRAP220 component of a thyroid hormone receptor-associated protein (TRAP) coactivator complex interacts directly with nuclear receptors in a ligand-dependent fashion. *Proc. Natl. Acad. Sci. USA* **95**, 7939–7944.

Received: 28 July 2005
Accepted: 30 August 2005

Differential contributions of Mesp1 and Mesp2 to the epithelialization and rostro-caudal patterning of somites

Yu Takahashi[1,*], Satoshi Kitajima[1], Tohru Inoue[1], Jun Kanno[1] and Yumiko Saga[2,*]

[1]Cellular & Molecular Toxicology Division, National Institute of Health Sciences, 1-18-1 Kamiyoga, Setagayaku, Tokyo 158-8501, Japan
[2]Division of Mammalian Development, National Institute of Genetics, Yata 1111, Mishima 411-8540, Japan
*Authors for correspondence (e-mail: yutak@nihs.go.jp and ysaga@lab.nig.ac.jp)

Accepted 29 November 2004

Development 132, 787-796
Published by The Company of Biologists 2005
doi:10.1242/dev.01597

Summary

Mesp1 and Mesp2 are homologous basic helix-loop-helix (bHLH) transcription factors that are co-expressed in the anterior presomitic mesoderm (PSM) just prior to somite formation. Analysis of possible functional redundancy of Mesp1 and Mesp2 has been prevented by the early developmental arrest of Mesp1/Mesp2 double-null embryos. Here we performed chimera analysis, using either Mesp2-null cells or Mesp1/Mesp2 double-null cells, to clarify (1) possible functional redundancy and the relative contributions of both Mesp1 and Mesp2 to somitogenesis and (2) the level of cell autonomy of Mesp functions for several aspects of somitogenesis. Both Mesp2-null and Mesp1/Mesp2 double-null cells failed to form initial segment borders or to acquire rostral properties, confirming that the contribution of Mesp1 is minor during these events. By contrast, Mesp1/Mesp2 double-null cells contributed to neither epithelial somite nor dermomyotome formation, whereas Mesp2-null cells partially contributed to incomplete somites and the dermomyotome. This indicates that Mesp1 has a significant role in the epithelialization of somitic mesoderm. We found that the roles of the Mesp genes in epithelialization and in the establishment of rostral properties are cell autonomous. However, we also show that epithelial somite formation, with normal rostro-caudal patterning, by wild-type cells was severely disrupted by the presence of Mesp mutant cells, demonstrating non-cell autonomous effects and supporting our previous hypothesis that Mesp2 is responsible for the rostro-caudal patterning process itself in the anterior PSM, via cellular interaction.

Key words: Somitogenesis, Epithelial-mesenchymal conversion, Mesp2, Chimera analysis, Mouse

Introduction

Somitogenesis is not only an attractive example of metameric pattern formation but is also a good model system for the study of morphogenesis, particularly epithelial-mesenchymal interconversion in vertebrate embryos (Gossler and Hrabe de Angelis, 1997; Pourquié, 2001). The primitive streak, or tailbud mesenchyme, supplies the unsegmented paraxial mesoderm, known as presomitic mesoderm (PSM). Mesenchymal cells in the PSM undergo mesenchymal-epithelial conversion to form epithelial somites in a spatially and temporally coordinated manner. Somites then differentiate, in accordance with environmental cues from the surrounding tissues, into dorsal epithelial dermomyotome and ventral mesenchymal sclerotome (Borycki and Emerson, 2000; Fan and Tessier Lavigne, 1994). Hence, the series of events that occur during somitogenesis provide a valuable example of epithelial-mesenchymal conversion. The dermomyotome gives rise to both dermis and skeletal muscle, whereas the sclerotome forms cartilage and bone in both the vertebrae and the ribs. Each somite is subdivided into two compartments, the rostral (anterior) and caudal (posterior) halves. This rostro-caudal polarity appears to be established just prior to somite formation (Saga and Takeda, 2001).

Mesp1 and Mesp2 are closely related members of the basic helix-loop-helix (bHLH) family of transcription factors but share significant sequence homology only in their bHLH regions (Saga et al., 1996; Saga et al., 1997). During development of the mouse embryo, both *Mesp1* and *Mesp2* are specifically expressed in the early mesoderm just after gastrulation and in the paraxial mesoderm during somitogenesis. Mesp1/Mesp2 double-null embryos show defects in early mesodermal migration and thus fail to form most of the embryonic mesoderm, leading to developmental arrest (Kitajima et al., 2000). Mesp1-null embryos exhibit defects in single heart tube formation, due to a delay in mesodermal migration, but survive to the somitogenesis stage (Saga et al., 1999), suggesting that there is some functional redundancy, i.e. compensatory functions of Mesp2 in early mesoderm. During somitogenesis, both *Mesp1* and *Mesp2* are expressed in the anterior PSM just prior to somite formation. Although we have shown that Mesp2, but not Mesp1, is essential for somite formation and the rostro-caudal patterning of somites (Saga et al., 1997), a possible functional redundancy between Mesp1 and Mesp2 has not yet been clearly established.

To further clarify the contributions of Mesp1 and Mesp2 to somitogenesis, analysis of Mesp1/Mesp2 double-null embryos

is necessary, but because of the early mesodermal defects already described, these knockout embryos lack a paraxial mesoderm, which prevents any analysis of somitogenesis. We therefore adopted a strategy that utilized chimera analysis. As we have reported previously, the early embryonic lethality of a Mesp1/Mesp2 double knockout is rescued by the presence of wild-type cells in a chimeric embryo, but the double-null cells cannot contribute to the cardiac mesoderm (Kitajima et al., 2000). This analysis, however, focused only on early heart morphogenesis and did not investigate the behavior of Mesp1/Mesp2 double-null cells in somitogenesis. In this report, we focus upon somitogenesis and compare two types of chimeras using either Mesp1/Mesp2 double-null cells or Mesp2-null cells to investigate Mesp1 function during somitogenesis.

Another purpose of our chimera experiments was to elucidate the cell autonomy of Mesp functions. In the process of somite formation, mesenchymal cells in the PSM initially undergo epithelialization at the future segment boundary, independently of the already epithelialized dorsal or ventral margin of the PSM (Sato et al., 2002). Epithelial somite formation is disrupted in the Mesp2-null embryo, indicating that Mesp2 is required for epithelialization at the segment boundary. Although Mesp products are nuclear transcription factors and their primary functions must therefore be cell autonomous (transcriptional control of target genes), it is possible that the roles of Mesp2 in epithelialization are mediated by the non-cell autonomous effects of target genes. We therefore asked whether the defects in Mesp2-null cells during epithelialization could be rescued by the presence of surrounding wild-type cells. Additionally, we would expect to find that the role of Mesp2 in establishing rostro-caudal polarity is rescued in a similar way.

Our analysis suggests that Mesp1 and Mesp2 have redundant functions and are both cell-autonomously involved in the epithelialization of somitic mesoderm. In addition, our results highlight some non-cell autonomous effect of Mesp2-null and Mesp1/Mesp2-null cells.

Materials and methods

Generation of chimeric embryos

As described previously (Kitajima et al., 2000), chimeric embryos were generated by aggregating 8-cell embryos of wild-type mice (ICR) with those of mutant mice that were genetically marked with the *ROSA26* transgene (Zambrowicz et al., 1997). Mesp1/Mesp2 double-null embryos were generated by crossing *wko-del (+/–)* and *Mesp1(+/–)/Mesp2(+/cre)* mice as described previously (Kitajima et al., 2000). This strategy enables us to distinguish chimeric embryos derived from homozygous embryos, which have two different mutant alleles, from those derived from heterozygous embryos. Likewise, Mesp2-null embryos were generated by crossing *P2v1(+/–)* mice (Saga et al., 1997) and *P2GFP (+/gfp)* mice (Y.S. and S.K., unpublished) that were also labeled with the *ROSA26* locus. The genotype of the chimeric embryos was determined by PCR using yolk sac DNA.

Histology, histochemistry and gene expression analysis

The chimeric embryos were fixed at 11 days postcoitum (dpc) and stained in X-gal solution for the detection of β-galactosidase activity, as described previously (Saga et al., 1999). For histology, samples stained by X-gal were postfixed with 4% paraformaldehyde, dehydrated in an ethanol series, embedded in plastic resin (Technovit 8100, Heraeus Kulzer) and sectioned at 3 μm. The methods used for gene expression analysis by in-situ hybridization of whole-mount samples and frozen sections and skeletal preparation by Alcian Blue/Alizarin Red staining were described previously (Saga et al., 1997; Takahashi et al., 2000). Probes for in-situ hybridization for *Uncx4.1* (Mansouri et al., 1997; Neidhardt et al., 1997), *Delta-like 1 (Dll1)* (Bettenhausen et al., 1995) and *Paraxis* (Burgess et al., 1995) were kindly provided by Drs Peter Gruss, Achim Gossler and Alan Rawls, respectively. A probe for *EphA4* (Nieto et al., 1992) was cloned by PCR. For detection of actin filaments, frozen sections were stained with AlexaFluor 488-conjugated phalloidin (Molecular Probes) according to the manufacturer's protocol.

Results

Possible functional redundancy and different contributions of Mesp1 and Mesp2 in somitogenesis

During somitogenesis, both *Mesp1* and *Mesp2* are expressed in the anterior PSM just prior to somite formation and their expression domains overlap (Fig. 1A). Mesp1-null embryos form morphologically normal somites and show normal rostro-caudal patterning within each somite (Fig. 1B,E-H), indicating that Mesp1 is not essential for somitogenesis. By contrast, Mesp2 is essential for both the formation and rostro-caudal patterning of somites, as Mesp2-null embryos have no epithelial somites and lose rostral half properties, resulting in caudalization of the entire somitic mesoderm (Saga et al., 1997) (Fig. 1C,D).

Although somite formation and rostro-caudal patterning is disrupted in the Mesp2-null embryo, histological differentiation into dermomyotome and sclerotome is not affected. It is noteworthy that the Mesp2-null embryo still forms disorganized dermomyotomes without forming epithelial somites (Saga et al., 1997). As *Mesp1* is expressed at normal levels in the PSM of Mesp2-null embryos (Fig. 1C,D), it is possible that Mesp1 functions to rescue some aspects of somitogenesis in the Mesp2-null embryo. In order to further clarify the contributions of both Mesp1 and Mesp2 during somitogenesis, we therefore generated chimeric embryos with either Mesp2-null cells or Mesp1/Mesp2 double-null cells and compared the behavior of mutant cells during somitogenesis (Fig. 2).

Mesp2-null cells tend to be eliminated from the epithelial somite and the dermomyotome, but can partially contribute to both of these structures

We first generated Mesp2-null chimeric embryos (*Mesp2*$^{-/-}$ with *Rosa26*: wild) to analyze cell autonomy of Mesp2 function during somitogenesis. The control chimeric embryo (*Mesp2*$^{+/-}$ with *Rosa26*: wild) showed normal somitogenesis and a random distribution of X-gal stained cells (Fig. 3A). The Mesp2-null chimeric embryos formed abnormal somites that exhibited incomplete segmentation (Fig. 3B), but histological differentiation of dermomyotome and sclerotome was observed. Within the incomplete somite, X-gal-stained Mesp2-null cells were mainly localized in the rostral and central regions, surrounded by wild-type cells at the dorsal, ventral and caudal sides (Fig. 3B). The surrounding wild-type cells, however, did not form an integrated epithelial sheet, but consisted of several epithelial cell clusters. Such trends were more obviously observed in other sections, where wild-type cells were found to form multiple small epithelial clusters (Fig.

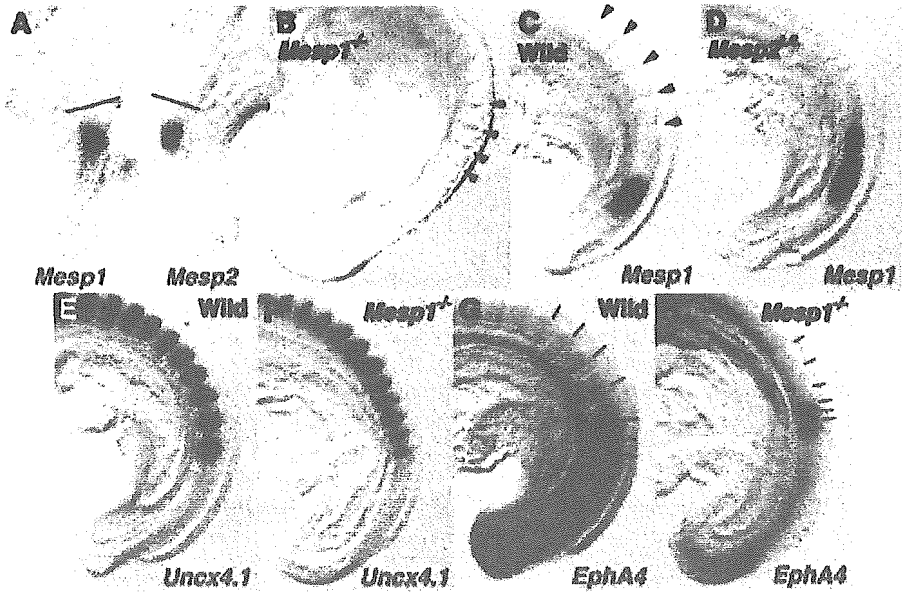

Fig. 1. *Mesp1* and *Mesp2* are co-expressed in the anterior PSM but have differing roles in somitogenesis. (A) Overlapping expression of *Mesp1* and *Mesp2* is revealed by in-situ hybridization using the left and right halves of the same embryo. The lines show most recently formed somite boundaries. (B-C) A Mesp1-null embryo (B) shows the same normal somite formation as a wild-type embryo (C). Arrowheads indicate somite boundaries. (D) In Mesp2-null embryos, no somite formation is observed but *Mesp1* is expressed at comparable levels to wild type, although its expression is anteriorly extended and blurred. (E-H) Mesp1-null embryos show normal rostro-caudal patterning of somites. (E,F) Expression of a caudal half marker, *Uncx4.1*. (G,H) Expression of a rostral half marker, *EphA4*. The lines indicate presumptive or formed somite boundaries and the dotted line indicates approximate position of somite half boundary.

3C,D). Mesp2-null cells tended to be eliminated from the epithelial clusters, although they were partially integrated into these structures (blue arrows in Fig. 3C,D). Likewise, small numbers of Mesp2-null cells were found to contribute to the dermomyotome (Fig. 3E,F). Mesp2-null cells also appeared to form the major part of the sclerotome.

Mesp2 is required for the cell-autonomous acquisition of rostral properties

We have previously demonstrated that suppression by Mesp2

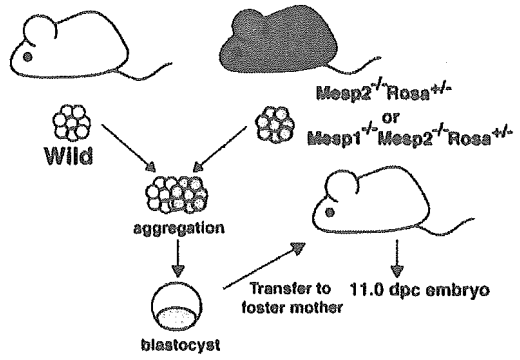

Fig. 2. Schematic representation of chimera analysis method. Either Mesp2-null or Mesp1/Mesp2 double-null embryos, genetically labeled with *Rosa* locus, were aggregated with wild-type embryos at the 8-cell stage, and the resulting chimeras were subjected to analysis at 11.0 dpc.

of the caudal genes *Dll1* and *Uncx4.1* in presumptive rostral half somites is a crucial event in the establishment of the rostro-caudal pattern of somites (Saga et al., 1997; Takahashi et al., 2000). As Mesp2-null embryos exhibit caudalization of somites, Mesp2-null cells are predicted to be unable to express rostral properties. Hence, Mesp2-null cells are expected to distribute to the caudal region of each somite where the rostro-caudal patterns are rescued by wild-type cells in a chimeric embryo. In this context, the localization of Mesp2-null cells at the rostral side was an unexpected finding. We interpret this to mean that the rostral location of Mesp2-null cells is due to a lack of epithelialization functions (see Discussion).

To examine rostro-caudal properties in Mesp2-null cells, located in the rostral side, we analyzed the expression of a caudal half marker gene, *Uncx4.1* (Mansouri et al., 1997; Neidhardt et al., 1997). Analysis of adjacent sections revealed that *lacZ*-expressing Mesp2-null cells, localized at the rostral and central portion, ectopically expressed *Uncx4.1* (Fig. 4A-D). This strongly suggests that Mesp2-null cells cannot acquire rostral properties even if surrounded by wild-type cells, and that Mesp2 function is cell-autonomously required for the acquisition of rostral properties. We also observed that the small number of Mesp2-null cells distributed mostly to the caudal end of the dermomyotome (Fig. 3E,F) and that the expression pattern of *Uncx4.1* was normal in the dermomyotome (Fig. 4E,F). In the sclerotome, *lacZ*-expressing Mesp2-null cells often distributed to the rostral side, where expression of *Uncx4.1* was abnormally elevated (Fig. 4G,H). The vertebrae of the Mesp2-null chimeric fetus showed a partial fusion of the neural arches, which was reminiscent of

Mesp2-hypomorphic fetuses (Fig. 4I,J) (Nomura-Kitabayashi et al., 2002). Fusion of proximal rib elements was also observed (Fig. 4K,L).

Mesp1/Mesp2 double-null cells cannot contribute to the formation of epithelial somites or to the dermomyotome

To address the question of whether Mesp1, in addition to Mesp2, exhibits any function during somitogenesis, we next generated Mesp1/Mesp2 double-null chimeric embryos and compared them with the Mesp2-null chimeric embryos described in the previous sections. We first performed whole-mount X-gal staining of embryos at 11 dpc. In the control chimeric embryo, the X-gal-stained Mesp1/Mesp2 double-heterozygous cells distributed randomly throughout the embryonic body, including the somite region (Fig. 5A,C). By contrast, the Mesp1/Mesp2 double-null chimeric embryo displayed a strikingly uneven pattern of cellular distribution in the somite region. The X-gal stained Mesp1/Mesp2 double-null cells were localized at the medial part of embryonic tail and were not observed in the lateral part of the somite region (Fig. 5B,D). Histological examination of parasagittal sections further revealed obvious differences in the cellular contribution to somite formation (Fig. 5E,F). In the control chimeric embryo, Mesp1/Mesp2 double-heterozygous cells distributed randomly throughout the different stages of somitogenesis (PSM, somite, dermomyotome and sclerotome: Fig. 5E). In the Mesp1/Mesp2 double-null chimeric embryo, neither the initial segment border nor epithelial somites were formed, but histologically distinguishable dermomyotome-like and sclerotome-like compartments were generated (Fig. 5F). In addition, Mesp1/Mesp2 double-null cells and wild-type cells were randomly mixed in the PSM, whereas the dermomyotome-like epithelium consisted exclusively of wild-type cells and the sclerotome-like compartment consisted mostly of Mesp1/Mesp2 double-null cells. This suggests that either Mesp1 or Mesp2 is cell-autonomously required for the formation of epithelial somite and dermomyotome. These results also indicate that PSM cells with different characteristics are rapidly sorted during somite formation.

Subsequent examination of transverse sections confirmed the elimination of Mesp1/Mesp2 double-null cells from dermomyotome (Fig. 5G,H). In the mature somite region, the wild-type dermomyotome-like epithelium was found to form the myotome (my) (Fig. 5I,J). Furthermore, the ventral part of this dermomyotome-like epithelium became mesenchymal and appeared to contribute to the dorsal sclerotome (dsc), implying that this initial dermomyotome-like epithelium actually corresponds to the epithelial somite exclusively composed of wild-type cells (Fig. 5I,J). Fluorescent phalloidin staining revealed that the apical localization of actin filaments is limited to the dorsal compartments, which are occupied by wild-type cells in the Mesp1/Mesp2 double-null chimeric embryo (Fig. 5K,L), indicating the Mesp1/Mesp2 double-null cells cannot undergo epithelialization.

It is known that the bHLH transcription factor paraxis (Tcf15 – Mouse Genome Informatics), is required for the epithelialization of somite and

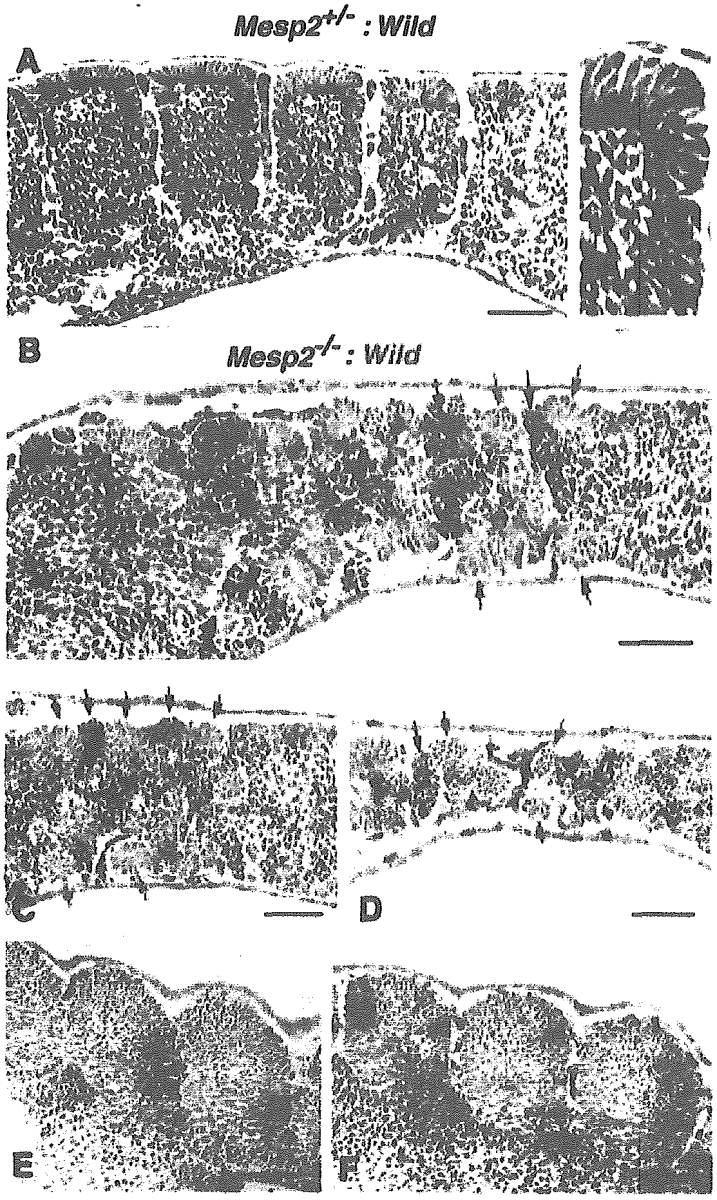

Fig. 3. Mesp2-null cells tend to be excluded from the epithelial region of the somites. (A) The control chimeric embryo undergoes normal somite formation and shows random distribution of labeled cells. The right panel is a high-power view of a somite. (B) In the Mesp2-null chimeric embryo, incompletely segmented somites are formed. Mesp2-null cells tend to be localized at the rostral and central region of these incomplete segments. Red arrows: wild-type cell clusters; blue arrows: Mesp2-null cell clusters. (C,D) Other sections indicating multiple small epithelial cell clusters (arrows). Note that Mesp2-null cells only partially contribute to the epithelial clusters (blue arrows). (E,F) A small number of Mesp2-null cells are distributed in the dermomyotome and are mostly localized at the caudal end. Scale bars: 100 μm.

dermomyotome (Burgess et al., 1995; Burgess et al., 1996). Although *Paraxis* expression is not affected in Mesp2-null embryos (data not shown), it is possible that it is influenced by the loss of both Mesp1 and Mesp2. We therefore examined the expression patterns of *Paraxis* in our Mesp1/Mesp2 double-null chimeras. In wild-type embryos *Paraxis* is initially expressed throughout the entire somite region (in both the prospective dermomyotomal and sclerotomal regions) in the anteriormost PSM and newly forming somites, and then localizes in the dermomyotomes (Burgess et al., 1995). The dorsal dermomyotomal epithelium, composed of wild-type cells, strongly expressed *Paraxis* in the chimeric embryo (Fig. 6A,B). In addition, adjacent sections revealed that *lacZ*-expressing Mesp1/Mesp2 double-null cells expressed *Paraxis* in the medial sclerotomal compartment (Fig. 6A,B, brackets). This suggests that *Paraxis* expression in the future sclerotomal region is independent of Mesp factors. However, at present we cannot exclude the possibility that the maintenance of *Paraxis* expression in the dermomyotome requires the functions of either Mesp1 or Mesp2.

Mesp1/Mesp2 double-null cells are incapable of acquiring rostral properties

To clarify the rostro-caudal properties of somites in our chimeric embryos, we examined the expression pattern of *Uncx4.1*. Control chimeric embryos exhibited a normal stripe pattern of *Uncx4.1* expression throughout the segmented somite region (Fig. 7A). By contrast, Mesp1/Mesp2 double-null chimeric embryos exhibited continuous *Uncx4.1* expression in the ventral sclerotomal region (Fig. 7B). This continuity was observed in the entire sclerotome-like compartment of the newly formed somite region and in the ventral sclerotome in the mature somite region. The caudal localization of *Uncx4.1* expression, however, was normal in the dermomyotome and the dorsal sclerotome, which consisted of wild-type cells (Fig. 5), even in Mesp1/Mesp2 double-null chimeras. This suggests that, like Mesp2-null cells, Mesp1/Mesp2 double-null cells are incapable of acquiring rostral properties. Since the mesoderm of Mesp1/Mesp2 double-null embryos lacks the expression of the major markers of paraxial mesoderm (Kitajima et al., 2000), and Mesp1/Mesp2 double-null cells do not exhibit histological features characteristic of epithelial somites in our current study, it is possible that Mesp1/Mesp2 double-null cells may lack paraxial mesoderm properties. However, the analysis of adjacent sections suggests that *lacZ*-expressing Mesp1/Mesp2 double-null cells themselves express *Uncx4.1*, a somite-specific marker (Fig. 7C,D), and they had also been found to have normal expression of *Paraxis* (Fig. 6A,B).

It is believed that the rostro-caudal pattern within somites and dermomyotomes is generated in the PSM and maintained in somites and dermomyotomes. We observed a normal rostro-caudal pattern in the dermomyotome (Fig. 7), although wild-type cells and Mesp1/Mesp2 double-null cells are mixed in the PSM (Fig. 5), of Mesp1/Mesp2 double-null chimeric embryos. As Mesp products are required for suppression of *Dll1* in the anterior PSM, a normal Dll1 stripe pattern cannot be formed if Mesp1/Mesp2 double-null cells are randomly distributed in

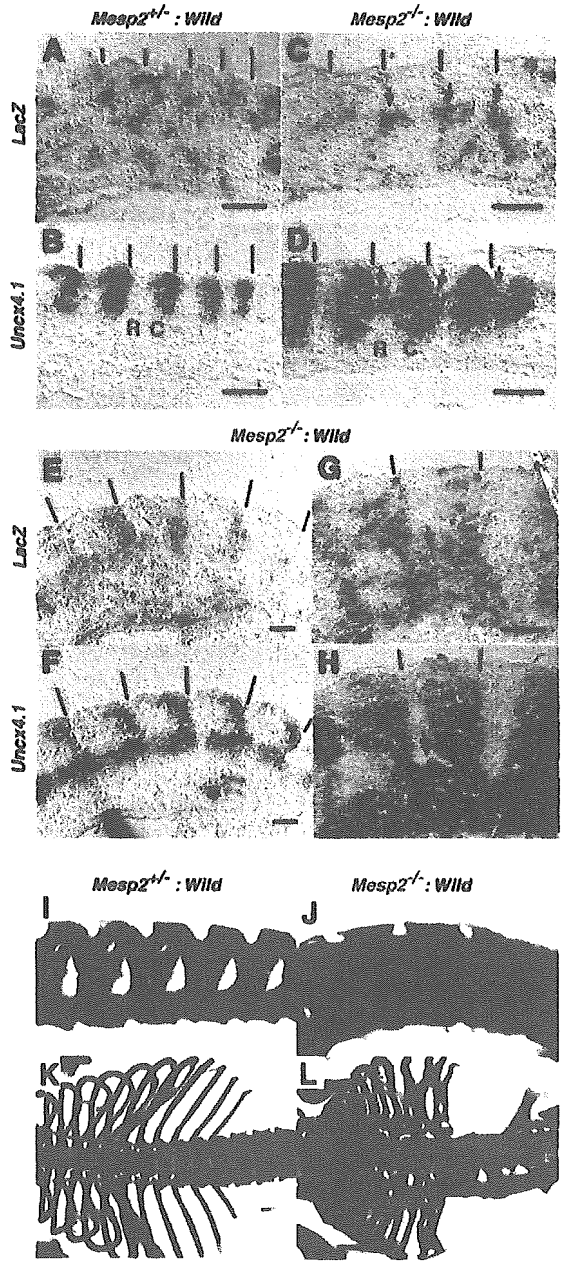

Fig. 4. Mesp2 function is cell autonomously required for rostral properties. (A-D) Expression of *lacZ* and *Uncx4.1* transcripts at the site of initial somite formation in control (A,B) and Mesp2-null (C,D) chimeric embryos. In the control, *lacZ*-expressing cells are randomly distributed and *Uncx4.1* expression is normal. In the Mesp2-null chimera, *lacZ*-expressing Mesp2-null cells at the rostral part of the incomplete segments (arrows in C) ectopically express *Uncx4.1* (arrows in D). Lines indicate somite boundaries. (E,F) In the dermomyotome, Mesp2-null cells are mostly localized at the caudal end, and the *Uncx4.1* expression pattern is normal. (G,H) In the sclerotome, the distribution of Mesp2-null cells results in expansion of *Uncx4.1* expression (arrows). (I) The control chimeric fetus shows normal vertebrae. (J) The Mesp2-null chimeric fetus exhibits partial fusion of the neural arches. (K) The control chimeric fetus shows normal ribs. (L) The Mesp2-null chimeric fetus shows proximal rib fusion. Scale bars: 100 μm. C, caudal compartment; R, rostral compartment.

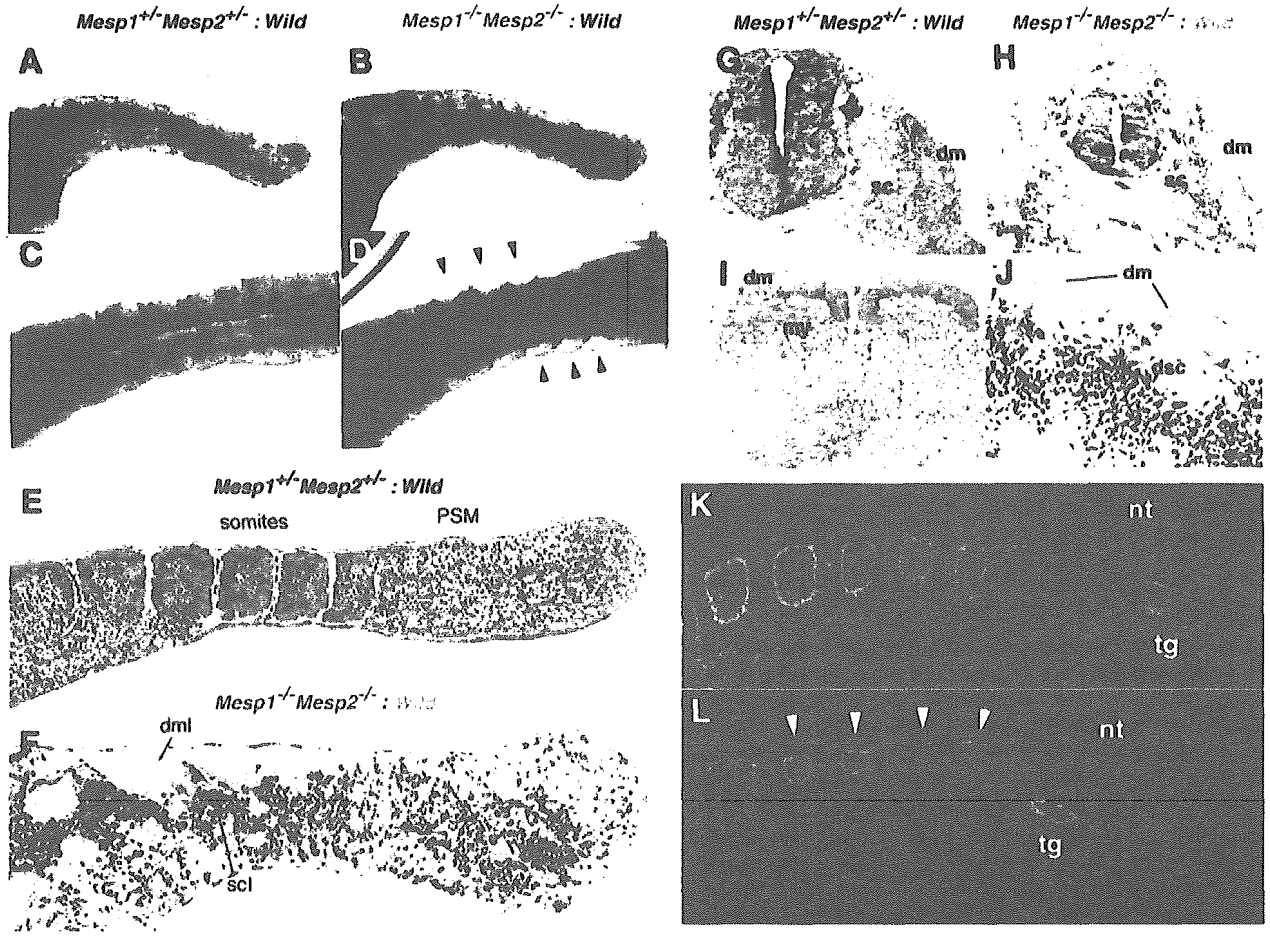

Fig. 5. Mesp1/Mesp2 double-null cells fail to contribute to epithelial somites or to the dermomyotome. (A-D) Tail regions from X-gal-stained whole-mount specimens of control (A,C) and double-null (B,D) chimeric embryos. (A,B) Lateral view. (C,D) Dorsal view. The blue double-heterozygous cells are randomly distributed in the control embryo, whereas the Mesp1/Mesp2 double-null cells are excluded from the lateral region of the somites (arrowheads in D). (E,F) Parasagittal sections of tails from chimeric embryos. (E) The labeled cells are randomly located in the control chimera. (F) The two types of cells are randomly mixed in the PSM, whereas the dermomyotome-like epithelium consisted exclusively of wild-type cells and the sclerotome-like compartment contained mostly Mesp1/Mesp2 double-null cells. Note that normal epithelial somites are not formed in this chimera. (G,H) Transverse sections show elimination of Mesp1/Mesp2 double-null cells from the dermomyotome. (I,J) The dermomyotome-like epithelium in the Mesp1/Mesp2 double-null chimeric embryo gives rise to dermomyotome, myotome (arrowhead in J) and the dorsal part of the sclerotome. Red arches indicate the inner surface of dermomyotome. (K,L) AlexaFluor 488-labeled phalloidin staining shows normal epithelialization of somites in the control chimera (K) and restriction of epithelialization in the dermomyotome-like compartment in the Mesp1/Mesp2 double-null chimera (L). dm, dermomyotome; dml, dermomyotome-like epithelium; dsc, dorsal part of the sclerotome; my, myotome; nt, neural tube; sc, sclerotome; scl, sclerotome-like compartment; tg, tail gut.

the anterior PSM. This is because 50% of cells cannot undergo suppression of Dll1 even in the future rostral half region. Therefore, our finding of a normal rostro-caudal pattern in the dermomyotome of double-null chimeras is surprising and raises the question of whether wild-type cells can be normally patterned in the presence of surrounding Mesp1/Mesp2 double-null cells. To determine how the rostro-caudal pattern in the dermomyotome is formed in the PSM, we examined the expression pattern of *Dll1* (Bettenhausen et al., 1995), the stripe expression profile of which is established in the anteriormost PSM via the function of Mesp2 (Takahashi et al., 2000). The *lac*Z-expressing Mesp1/Mesp2 double-null cells were subsequently found to be consistently localized in the sclerotome-like region, where *Dll1* expression was abnormally expanded (Fig. 6C,D). In the dermomyotome-like region, however, *Dll1* expression in the caudal half was normal. Intriguingly, strong *Dll1* expression in the anteriormost PSM was suppressed in a rostrally adjoining cell population, which is mainly occupied by wild-type cells (Fig. 6C,D, arrows). This implies that wild-type cells and Mesp1/Mesp2 double-null cells rapidly segregate at S–1 to S0, after which the rostro-caudal pattern of *Dll1* expression is formed in the partially segregated wild-type cell population but not in the randomly mixed cell population. In other words, the separation from Mesp1/Mesp2 double-null cells enabled normal rostro-caudal patterning of wild-type cells.

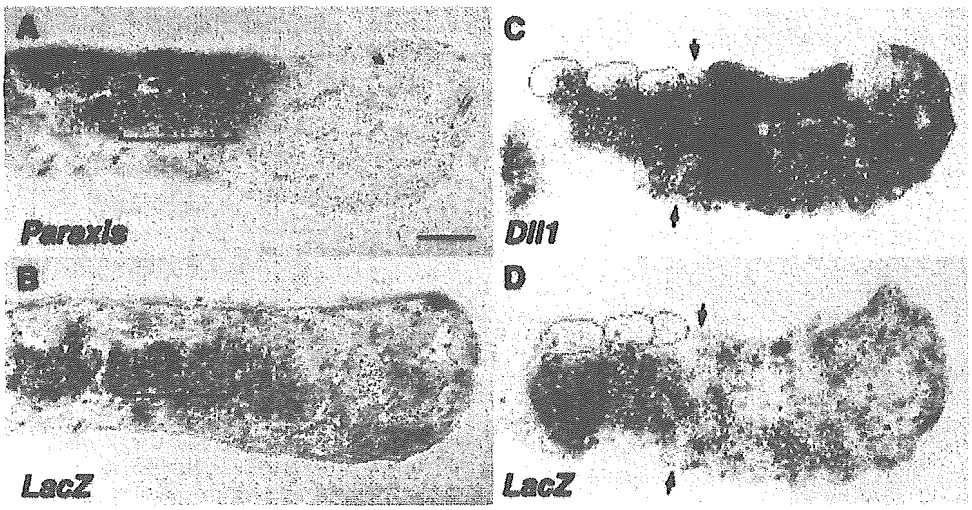

Fig. 6. (A,B) Mesp1/Mesp2 double-null cells express *Paraxis*. Adjacent parasagittal sections of the Mesp1/Mesp2 double-null chimeric embryo were stained for either *Paraxis* (A) or *lacZ* (B). Note that the expression domains of the two genes overlap in the medial sclerotomal region (brackets). (C,D) The rostro-caudal pattern in the dermomyotome is formed in a partially segregating wild-type cell population. Adjacent sections of the Mesp1/Mesp2 double-null chimeric embryos were stained for *Dll1* (C) or *lacZ* (D) mRNA. Red outlines demarcate the dorsal dermomyotome-like compartments. Note that suppression of *Dll1* expression occurs in a region mostly occupied by wild-type cells (arrows). Scale bar: 100 μm.

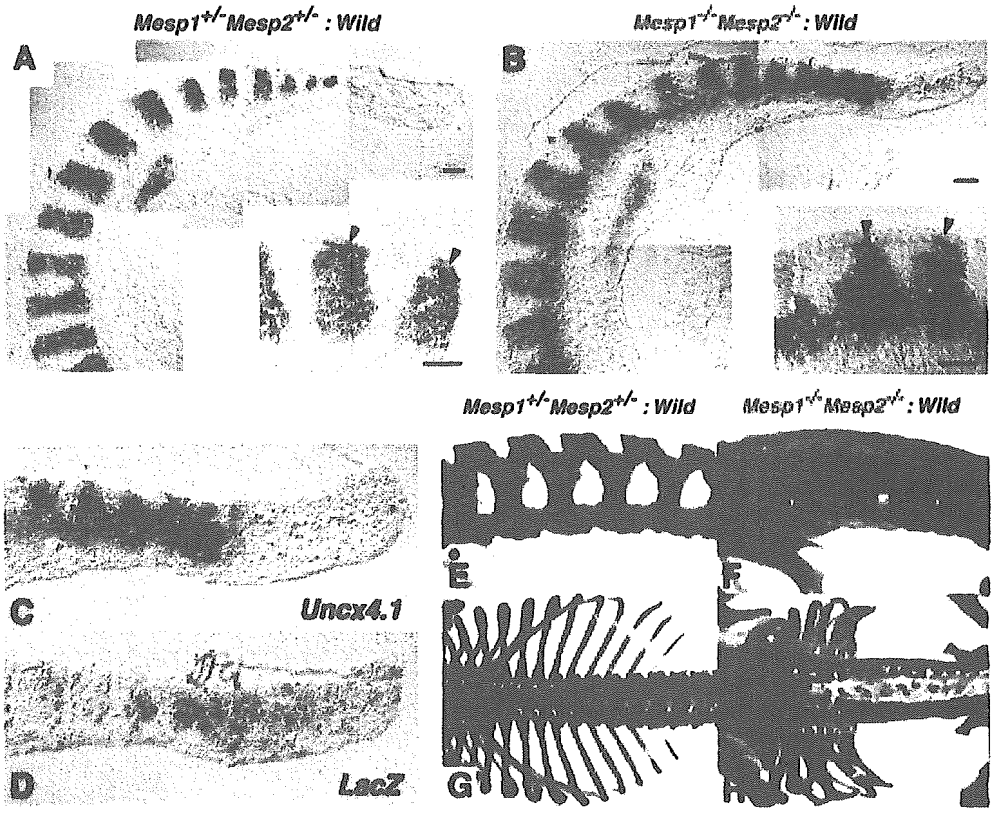

Fig. 7. Rostro-caudal patterning of the sclerotome is disrupted in Mesp1/Mesp2 double-null chimeric embryos. (A) The control chimeric embryos exhibit normal stripe patterns of *Uncx4.1* expression throughout the somite region. (B) The Mesp1/Mesp2 double-null chimeric embryos exhibit continuous *Uncx4.1* expression in the ventral sclerotomal region. Note that caudal localization of *Uncx4.1* expression is normal in the dermomyotome and dorsal sclerotome. The insets show a higher magnification of lumbar somites. (C,D) Adjacent sections showing that *lacZ*-expressing Mesp1/Mesp2 double-null cells express *Uncx4.1*. (E-H) The Mesp1/Mesp2 double-null chimeric fetus exhibits caudalization of the vertebrae and of the proximal ribs. (E) The control chimeric fetus shows normal metameric arrangement of the neural arches. (F) The Mesp1/Mesp2 double-null chimeric fetus shows severe fusion of the pedicles and the laminae of neural arches. (G) The control chimeric fetus has normal arrangement of ribs. (H) The double-null chimeric fetus shows severe fusion of the proximal elements of the ribs. Scale bars: 100 μm.

Mesp2-null fetuses display caudalized vertebrae with extensive fusion of the pedicles of neural arches and proximal elements of the ribs (Saga et al., 1997). The Mesp1/Mesp2 double-null chimeric fetuses also exhibited fusion of the pedicles of neural arches and the proximal ribs (Fig. 7E-H). Furthermore, the vertebrae of severe chimeric fetuses were indistinguishable from those of Mesp2-null fetuses. These observations indicate that Mesp1/Mesp2 double-null cells can differentiate into caudal sclerotome and possibly contribute to chondrogenesis.

Discussion

Mesp1 and Mesp2 not only exhibit similar expression patterns but also share common bHLH domains as transcription factors. Previous studies using gene replacement experiments (Saga, 1998) (Y.S. and S.K., unpublished) indicate that these genes can compensate for each other. However, the early lethality of double knockout mice hampered any further detailed analysis of somitogenesis. An obvious strategy to further elucidate the functions of Mesp1 and Mesp2 was, therefore, the generation of a conditional knockout allele for *Mesp2* in *Mesp1* disrupted cells in which the Cre gene is specifically activated in the paraxial mesoderm, which is now underway. Chimera analysis is also a powerful method as an alternative strategy. Comparisons of chimeras, composed of either Mesp2-null or Mesp1/Mesp2 double-null cells, made it possible to determine the contribution of Mesp1 to somitogenesis. Our results indicate that Mesp1 has redundant functions in the epithelialization of somitic mesoderm and additionally, by chimeric analysis, we were able to demonstrate the cell autonomy of Mesp1 and Mesp2 function during some critical steps of somitogenesis.

The relative contributions of Mesp1 and Mesp2 to somitogenesis

In Mesp1-null mice, epithelial somites with normal rostro-caudal polarity are generated, whereas Mesp2-null mice exhibit defects in both the generation of epithelial somites and the establishment of rostro-caudal polarity. Thus, it seems likely that Mesp2 function is both necessary and sufficient for somitogenesis. However, dermomyotome formation was observed, without normal segmentation, even in Mesp2-null mice. In view of the apparent redundant functions of Mesp1 and Mesp2 in somitogenesis, as demonstrated by our previous gene replacement study, it was possible that the Mesp1/Mesp2 double-null embryo would exhibit a much more severe phenotype in relation to somitogenesis. In our chimera analyses, both Mesp2-null and Mesp1/Mesp2 double-null cells exhibited complete caudalization of somitic mesoderm, indicating that Mesp1 function is not sufficient to rescue Mesp2 deficiency and restore rostro-caudal polarity. Likewise, both Mesp2-null and Mesp1/Mesp2 double-null cells were incapable of forming an initial segment boundary, showing that the contribution of Mesp1 is also minor during this process. By contrast, whereas Mesp1/Mesp2 double-null cells lacked any ability to epithelialize, Mesp2-null cells were occasionally integrated into epithelial somites and dermomyotome, indicating that the contribution of Mesp1 to epithelialization is significant and that Mesp1 can function in the absence of Mesp2 (Fig. 8). We therefore postulate that the epithelialization of dermomyotome, observed in Mesp2-null embryos, is dependent on Mesp1.

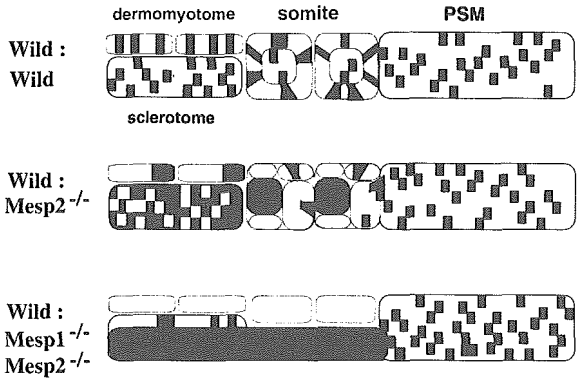

Fig. 8. A schematic summarization of the Mesp1/Mesp2 chimera experiments. Mesp1/Mesp2 double-null cells can contribute to neither epithelial somite nor dermomyotome formation, whereas Mesp2-null cells can partially contribute to both somites and dermomyotome. Red outlines indicate epithelialized tissues (epithelial somites, dermomyotomes and abnormal small clusters).

Mesp factors are cell autonomously required for epithelialization of somitic mesoderm but may also be non-cell autonomously required for morphological boundary formation

Conventional interpretations of the results of chimera analysis are generally based upon the regulative development of the vertebrate embryo and argue cell autonomy of specific gene functions in embryogenesis (Ciruna et al., 1997; Brown et al., 1999; Kitajima et al., 2000; Koizumi et al., 2001). Mesp1/Mesp2 double-null cells failed to form epithelial somites, even in the presence of surrounding wild-type cells. In addition, they were incapable of contributing to dermomyotome, where cell sorting occurs. This strongly suggests that Mesp factors are cell autonomously required for the epithelialization of somitic mesoderm. However, we also found striking non-cell autonomous effects of Mesp mutant cells on wild-type cell behaviors. That is, both types of Mesp mutant cell not only failed to undergo normal somitogenesis, but also inhibited the normal morphogenesis of wild-type cells. This implies that there are non-cell autonomous roles for Mesp factors in the establishment of the future somite boundary, as we will discuss further.

Initial epithelial somite formation is achieved by the mesenchymal-epithelial transition of cells located in the anterior PSM. A future somite boundary is established at a specific position in the PSM, followed by gap formation between the mesenchymal cell populations. Subsequently, cells located anterior to the boundary are epithelialized. This process is known to be mediated by an inductive signal from cells posterior to the boundary (Sato et al., 2002). Therefore, defects in epithelial somite formation can be explained in two principal ways: a lack of cellular ability to epithelialize (cell autonomous) and a lack of an inducing signal, which is produced in the anterior PSM by a mechanism mediated by Notch signaling (thus non-cell autonomous). In the case of chimeras of Mesp1/Mesp2 double-null cells, no local

boundary formed by locally distributed wild-type cells was observed, i.e. even a gap between wild-type cells was never observed in the mixture of Mesp1/Mesp2 double-null cells and wild-type cells. It is likely, therefore, that the wild-type cell population can form a boundary only after separation from Mesp1/Mesp2 double-null cells (Fig. 8). By contrast, some local boundaries between epithelial wild-type cell clusters were occasionally observed in chimeras with Mesp2-null cells. Considering that there is functional redundancy between these transcription factors, it is possible that either Mesp1 or Mesp2 is necessary for the formation of a signaling center or source of the putative inductive signal. Hence, we cannot exclude the possibility that the lack of Mesp function may affect non-cell autonomous generation of the inductive signal in the anterior PSM.

Formation of epithelial somites requires paraxis, which is a transcription factor (Burgess et al., 1996; Nakaya et al., 2004). We observed that Mesp1/Mesp2 double-null cells at the medial sclerotomal region expressed *Paraxis*, indicating that Mesp factors are not absolutely required for *Paraxis* expression. Defects in epithelial somite formation in paraxis-null embryos, with normal *Mesp2* expression (Johnson et al., 2001), and in Mesp2-null embryos, with normal *Paraxis* expression, imply that epithelial somite formation independently requires both gene functions.

Mesp2 is cell autonomously required for the acquisition of rostral properties

The distribution of Mesp2-null cells in the Mesp2-null chimeric embryos may appear somewhat paradoxical, as they are localized at the rostral side in the incomplete somites but at the caudal side in the dermomyotome. Initial localization at the rostral and central region, however, is likely to be due to the relative lack of epithelialization functions. In mammalian and avian embryos, mesenchymal-to-epithelial conversion of the PSM commences from the rostral side of the future somite boundary, i.e. the caudal margin of the presumptive somite (Duband et al., 1987). Epithelialization then proceeds anteriorly in the dorsal and ventral faces and in such a process, Mesp2-null cells, which are less able to participate in epithelialization, may therefore be pushed to the central and rostral sides. Thus, the majority of the Mesp2-null cells localize to the central, prospective sclerotomal region and a small number of them are integrated in the future dermomyotomal region. The incomplete somites then undergo reorganization into dermomyotome and sclerotome, and small numbers of Mesp2-null cells in the dermomyotome may be sorted out to the caudal end. Therefore, the apparently complex distribution pattern of Mesp2-null cells is likely to reflect a combination of defects in epithelialization and rostro-caudal patterning. In the incomplete segments of Mesp2-null chimeric embryos, the Mesp2-null cells fail to acquire rostral properties even when localized at the rostral side. Moreover, in the dermomyotome, where rostro-caudal patterning is rescued, Mesp2-null cells are mostly localized in the caudal region. These observations suggested that the requirement of Mesp2 for the acquisition of rostral properties is cell autonomous. Similarly, it has been reported that presenilin 1 (Psen1) is required for acquisition of caudal half properties (Takahashi et al., 2000; Koizumi et al., 2001) and that Psen1-null cells cannot contribute to the caudal half of somites in chimeric embryos, showing cell autonomous roles for Psen1 (Koizumi et al., 2001).

Mesp mutant cells affect the rostro-caudal patterning of somites due to the lack of cellular interaction with wild-type cells

In a previous study, we have shown that the rostro-caudal patterning of somites is generated by complex cellular interactions involved in positive and negative feedback pathways of Dll1-Notch and Dll3-Notch signaling, and regulation by Mesp2 in the PSM (Takahashi et al., 2003). In chimeras with either Mesp2-null or Mesp1/Mesp2 double-null cells, the mutant cells were distributed evenly and did not show any sorting bias in a rostro-caudal direction in the PSM. Since both Mesp2-null and Mesp1/Mesp2 double-null cells have the ability to form caudal cells, it is likely that if wild-type cells could occupy the rostral part of future somite regions and have the ability to sort in the PSM, a normal rostro-caudal patterning would be generated. We did not observe this, however, and conclude that the presence of mutant cells lacking Mesp factors must have disrupted normal cellular interactions via Notch signaling. Thus these non-cell-autonomous effects of our mutant cells are strongly supportive of our previous contention that rostro-caudal pattering is generated by cellular interactions via Notch signaling.

We thank Mariko Ikumi, Seiko Shinzawa, Eriko Ikeno and Shinobu Watanabe for general technical assistance. This work was supported by Grants-in-Aid for Science Research on Priority Areas (B) and the Organized Research Combination System of the Ministry of Education, Culture, Sports, Science and Technology, Japan.

References

Bettenhausen, B., Hrabe de Angelis, M., Simon, D., Guénet, J.-L. and Gossler, A. (1995). Transient and restricted expression during mouse embryogenesis of Dll1, a murine gene closely related to *Drosophila* Delta. *Development* **121**, 2407-2418.

Borycki, A. G. and Emerson, C. P., Jr (2000). Multiple tissue interactions and signal transduction pathways control somite myogenesis. *Curr. Top. Dev. Biol.* **48**, 165-224.

Brown, D., Wagner, D., Li, X., Richardson, D. A. and Olson, E. N. (1999). Dual role of the basic helix-loop-helix transcription factor scleraxis in mesoderm formation and chondrogenesis during mouse embryogenesis. *Development* **126**, 4317-4329.

Burgess, R., Cserjesi, P., Ligon, K. L. and Olson, E. N. (1995). Paraxis: a basic helix-loop-helix protein expressed in paraxial mesoderm and developing somites. *Dev. Biol.* **168**, 296-306.

Burgess, R., Rawls, A., Brown, D., Bradley, A. and Olson, E. N. (1996). Requirement of the *paraxis* gene for somite formation and musculoskeletal patterning. *Nature* **384**, 570-573.

Ciruna, B. G., Schwartz, L., Harpal, K., Yamaguchi, T. P. and Rossant, J. (1997). Chimeric analysis of *fibroblast growth factor receptor-1 (Fgfr1)* function: a role for FGFR1 in morphogenetic movement through the primitive streak. *Development* **124**, 2829-2841.

Duband, J. L., Dufour, S., Hatta, K., Takeichi, M., Edelman, G. M. and Thiery, J. P. (1987). Adhesion molecules during somitogenesis in the avian embryo. *J. Cell Biol.* **104**, 1361-1374.

Fan, C. M. and Tessier Lavigne, M. (1994). Patterning of mammalian somites by surface ectoderm and notochord: Evidence for sclerotome induction by a hedgehog homolog. *Cell* **79**, 1175-1186.

Gossler, A. and Hrabe de Angelis, M. (1997). Somitogenesis. *Curr. Top. Dev. Biol.* **38**, 225-287.

Johnson, J., Rhee, J., Parsons, S. M., Brown, D., Olson, E. N. and Rawls, A. (2001). The anterior/posterior polarity of somites is disrupted in Paraxis-deficient mice. *Dev. Biol.* **229**, 176-187.

Kitajima, S., Takagi, A., Inoue, T. and Saga, Y. (2000). MesP1 and MesP2

are essential for the development of cardiac mesoderm. *Development* **127**, 3215-3226.

Koizumi, K., Nakajima, M., Yuasa, S., Saga, Y., Sakai, T., Kuriyama, T., Shirasawa, T. and Koseki, H. (2001). The role of presenilin 1 during somite segmentation. *Development* **128**, 1391-1402.

Mansouri, A., Yokota, Y., Wehr, R., Copeland, N. G., Jenkins, N. A. and Gruss, P. (1997). Paired-related murine homeobox gene expressed in the developing sclerotome, kidney, and nervous system. *Dev. Dyn.* **210**, 53-65.

Nakaya, Y., Kuroda, S., Katagiri, Y. T., Kaibuchi, K. and Takahashi, Y. (2004). Mesenchymal-epithelial transition during somitic segmentation is regulated by differential roles of Cdc42 and Rac1. *Dev. Cell* **7**, 425-438.

Neidhardt, L. M., Kispert, A. and Herrmann, B. G. (1997). A mouse gene of the paired-related homeobox class expressed in the caudal somite compartment and in the developing vertebral column, kidney and nervous system. *Dev. Genes Evol.* **207**, 330-339.

Nieto, M. A., Gilardi-Hebenstreit, P., Charnay, P. and Wilkinson, D. G. (1992). A receptor protein tyrosine kinase implicated in the segmental patterning of the hindbrain and mesoderm. *Development* **116**, 1137-1150.

Nomura-Kitabayashi, A., Takahashi, Y., Kitajima, S., Inoue, T., Takeda, H. and Saga, Y. (2002). Hypomorphic *Mesp* allele distinguishes establishment of rostro-caudal polarity and segment border formation in somitogenesis. *Development* **129**, 2473-2481.

Pourquié, O. (2001). Vertebrate somitogenesis. *Annu. Rev. Cell. Dev. Biol.* **17**, 311-350.

Saga, Y. (1998). Genetic rescue of segmentation defect in MesP2-deficient mice by MesP1 gene replacement. *Mech. Dev.* **75**, 53-66.

Saga, Y. and Takeda, H. (2001). The making of the somite: molecular events in vertebrate segmentation. *Nat. Rev. Genet.* **2**, 835-845.

Saga, Y., Hata, N., Kobayashi, S., Magnuson, T., Seldin, M. and Taketo, M. M. (1996). MesP1: A novel basic helix-loop-helix protein expressed in the nascent mesodermal cells during mouse gastrulation. *Development* **122**, 2769-2778.

Saga, Y., Hata, N., Koseki, H. and Taketo, M. M. (1997). *Mesp2*: a novel mouse gene expressed in the presegmented mesoderm and essential for segmentation initiation. *Genes Dev.* **11**, 1827-1839.

Saga, Y., Miyagawa-Tomita, S., Takagi, A., Kitajima S., Miyazaki, J. and Inoue, T (1999). MesP1 is expressed in the heart precursor cells and required for the formation of a single heart tube. *Development* **126**, 3437-3447.

Sato, Y., Yasuda, K. and Takahashi, Y. (2002). Morphological boundary forms by a novel inductive event mediated by Lunatic fringe and Notch during somitic segmentation. *Development* **129**, 3633-3644.

Takahashi, Y., Koizumi, K., Takagi, A., Kitajima, S., Inoue, T., Koseki, H. and Saga, Y. (2000). Mesp2 initiates somite segmentation through the Notch signalling pathway. *Nat. Genet.* **25**, 390-396.

Takahashi, Y., Inoue, T., Gossler, A. and Saga, Y. (2003). Feedback loops comprising Dll1, Dll3 and Mesp2, and differential involvement of Psen1 are essential for rostrocaudal patterning of somites. *Development* **130**, 4259-4268.

Zambrowicz, B. P., Imamoto, A., Fiering, S., Herzenberg, L. A., Kerr, W. G. and Soriano, P. (1997). Disruption of overlapping transcripts in the ROSA beta geo 26 gene trap strain leads to widespread expression of beta-galactosidase in mouse embryos and hematopoietic cells. *Proc. Natl. Acad. Sci. USA* **94**, 3789-3794.

ANTICANCER RESEARCH *25*: 1881-1888 (2005)

Down-regulation of Skp2 is Correlated with p27-associated Cell Cycle Arrest Induced by Phenylacetate in Human Prostate Cancer Cells

TAKUJI SHIBAHARA, TAKEHISA ONISHI, OMAR E. FRANCO, KIMINOBU ARIMA and YOSHIKI SUGIMURA

Department of Urology, Mie University Facutly of Medicine, Tsu, Mie, Japan

Abstract. *We have demonstrated that phenylacetate(PA)-induced cell cycle arrest in human prostate cancer is mediated by increase of p27. In this study, we further investigated the mechanism of PA-induced p27 expression in prostate cancer cells (LNCaP, androgen-independent LNCaP [AIDL] and PC-3). A striking decrease in Skp2 mRNA and protein expression and reciprocal increase in p27 protein level were observed in three PA-treated prostate cancer cells. Interestingly, reduction of phospho-Akt and up-regulation of p27 mRNA levels were observed only in PC-3 cells. No significant differences were found in phospho-Akt and p27 mRNA levels in LNCaP and AIDL. In vitro ubiquitination assay showed a decreased p27 ubquitination in PA-treated prostate cancer cells. Our results suggest that PA attenuated Skp2 expression, thereby inhibiting ubiquitination and promoting p27 accumulation in all three prostate cancer cell lines. Therapeutic strategies designed to reduce Skp2 may clinically play an important role in the treatment of both androgen-sensitive and hormone-refractory prostate cancer.*

Androgen ablation therapy is the standard for advanced prostate cancer (1). This therapy is initially very effective, however, most advanced, especially metastatic cancers, tend to be resistant to androgen deprivation strategies during continuous hormone depletion therapy. Once in the state of androgen independence, this therapy is no longer effective (2), and no other therapy, including cytotoxic chemotherapy, is available at present. Therefore, novel therapies for hormone-refractory prostate cancer are warranted.

Correspondence to: Takehisa Onishi, M.D., Department of Urology, Mie University Faculty of Medicine, 2-174 Edobashi, Tsu, Mie 514-8507, Japan. Tel: 81-59-232-1111, ext. 6456, Fax: 81-59-231-5203, e-mail: takehisa@clin.medic.mie-u.ac.jp

Key Words: Phenylacetate, prostate cancer, Skp2, p27.

We noted that phenylacetate (PA), a physiological product of phenylalanine metabolism, is present at micromolar levels in human plasma (3) and is conjugated to glutamine in the liver by phenylacetyl coenzyme A to form phenylacetylglutamine. Based on this feature, it has been used safely to treat children with inborn errors of urea synthesis and also in patients with hyperammonemia (4, 5). PA has been shown to be a nontoxic differentiation activator and a new class of tumor growth-inhibitory compounds. It has been demonstrated that treatment with millimolar concentrations of PA resulted in cytostasis, growth inhibition and differentiation in various hematological and solid neoplasms, including prostate cancer (6-12).

Our previous study showed that PA induced cell cycle arrest at G1-S transition, and reduced phosphorylation of the retinoblastoma protein (pRb) and cyclin-dependent kinase 2 (CDK2) activity by increasing p27 protein levels in human prostate cancer cells (13). The results implicate that PA-induced growth inhibition is mainly *via* regulation of p27 status in prostate cancer cells. p27 is a member of the Kip1/Cip1 family of cyclin-dependent kinase inhibitors (CDKIs), which negatively regulates cyclin-CDK complexes at the G1-S transition, thus inhibiting entry into the S-phase of the cell cycle. It has been shown that low levels of p27 are correlated with tumor grade, recurrence rate and prognosis in several cancers (14-18).

The abundance of p27 is regulated by a post-translational mechanism, mainly through the ubiquitin-mediated protein degradation system (19). This ubiquitination is performed by S-phase kinase-associated protein 2 (Skp2), which is a member of the F-box family (20). Binding of p27 to Skp2 requires its phosphorylation at threonine residue 187 by cyclin-CDK complexes, and this binding is greatly increased by the CDK subunit 1 (Cks1) (21). Previous studies also demonstrated that the transcription of p27 is activated by AFX (22), which is negatively regulated by Akt (23-26). Akt is a critical regulator of cell proliferation and survival and induces cell invasiveness